
Article

Simulation of Organic Liquid Products Deoxygenation by Multistage Countercurrent Absorber/Stripping Using CO₂ as Solvent with Aspen-HYSYS: Process Modeling and Simulation

Manoel Raimundo dos Santos Jr¹, Elinéia Castro Costa¹, Caio Campos Ferreira¹, Lucas Pinto Bernar¹, Marcilene Paiva da Silva², Andréia de Andrade Mâncio³, Marcelo Costa Santos², Sílvio Alex Pereira da Mota¹, Douglas Alberto Rocha de Castro¹, Sergio Duvoisin Jr.³, Luiz Eduardo Pizarro Borges⁴, Marilena Emmi Araújo² and Nélío Teixeira Machado^{1,5*}

¹ Graduate Program of Natural Resources Engineering of Amazon; Rua Augusto Corrêa N° 1, Campus Profissional-UFFPA, Belém-Pará-Brazil, CEP: 66075-110, manoeljr@ufpa.br (M.R. d. S. Jr.); elinéia.costa.ec@gmail.com (E.C.C.); caiocf7@hotmail.com (C.C.F.); lucas.bernar7@gmail.com (L.P.B.); dedei-aam@yahoo.com.br (A.d. A. M.); marcelo.santos@ufpa.edu.br (M.C.S.); silviomota@unifesp.edu.br (S.A.P.d.M.); douglascastro87@hotmail.com (D.A.R.d.C.);

² Graduate Program of Chemical Engineering; Rua Augusto Corrêa N° 1, Campus Profissional-UFFPA, Belém-Pará-Brazil, CEP: 66075-900, arci_paiva@hotmail.com (M.P.d.S.); meaaraujo@gmail.com (M.E.A.)

³ Faculty of Chemical Engineering, Universidade do Estado do Amazonas-UEA, Avenida Darcy Vargas N° 1200, Manaus 69050-020, Brazil; sjunior@uea.edu.br (S.D.Jr.)

⁴ Laboratory of Catalyst Preparation and Catalytic Cracking, Section of Chemical Engineering, Instituto Militar de Engenharia-IME, Praça General Tibúrcio N° 80, Rio de Janeiro 22290-270, Brazil; luiz@ime.eb.br (L.E.P.B.)

⁵ Faculty of Sanitary and Environmental Engineering, Rua Augusto Corrêa N° 1, Campus Profissional-UFFPA, Belém-Pará-Brazil, CEP: 66075-900; faesa@ufpa.br

* Correspondence: machado@ufpa.br; Tel.: +55-91-984620325

Abstract: In this work, the deoxygenation of organic liquid products (OLP) obtained by thermal catalytic cracking of palm oil at 450 °C, 1.0 atmosphere, with 10% (wt.) Na₂CO₃ as catalyst, in multistage countercurrent absorber columns using supercritical carbon dioxide (SC-CO₂) as solvent, with Aspen-HYSYS process simulator was systematically investigated. In a previous study, the thermodynamic data basis and EOS modeling necessary to simulate the deoxygenation of OLP has been presented [Molecules 2021, 26, 4382. <https://doi.org/10.3390/molecules26144382>]. This work address a new flowsheet, consisting of 03 absorber columns, 10 expansions valves, 10 flash drums, 08 heat exchanges, 01 pressure pump, and 02 make-up of CO₂, aiming to improve the deacidification of OLP. The simulation was performed at 333 K, 140 bar, and (S/F) = 17; 350 K, 140 bar, and (S/F) = 38; 333 K, 140 bar, and (S/F) = 25. The simulation shows that 81.49% of OLP could be recovered and the concentrations of hydrocarbons in the extracts of absorber-01 and absorber-02 were 96.95 and 92.78% (wt.) in solvent-free basis, while the bottom stream of absorber-03 was enriched in oxygenates compounds with concentrations up to 32.66% (wt.) in solvent-free basis, showing that organic liquid products (OLP) was deacidified and SC-CO₂ was able to deacidify OLP and to obtain fractions with lower olefins content. The best deacidifying conditions was obtained at 333 K, 140 bar, and (S/F) = 17.

Keywords: OLP; Deoxygenation, Absorber columns, Process flowsheet, Process Simulation; Aspen-HYSYS.

1. Introduction

Thermal catalytic cracking is one of the most promising processes to convert and/or transform vegetable oils [1-17], residual oils [18-25], animal fats [26-28], mixtures of car-

boxylic acids [28-33], soaps of carboxylic acids [34-35], scum, grease, fats [36-38], and residual animal fat [27], into liquid hydrocarbons based biofuels [39]. This process has the objective to obtain liquid hydrocarbons for use as fuels [1-2, 4-5, 8, 10-11, 13-18, 20, 22, 26-39].

The reaction products obtained by thermochemical transformation of vegetable oils, residual oils, animal fats, mixture of carboxylic acids, scum, grease, and fats, soaps of carboxylic acids, and residual animal fats include gaseous and liquid fuels, water, aqueous acid phase, and coke [6-8, 10, 16-19, 23, 28-30, 35-38]. The physicochemical properties and chemical composition of organic liquid products depends on the compositional and physicochemical properties of raw material, process temperature, residence time, mode of operation (fluidized bed reactor, sludge bed reactor, etc.), presence of water in the raw material, and catalyst nature (acid, basic) selectivity [4, 6-8, 11-14, 17-20, 22-25, 28, 32-33, 36].

The organic liquid products are composed by alkanes, alkenes, ring-containing alkanes, ring-containing alkenes, cyclo-alkanes, cyclo-alkenes, and aromatics [4, 8, 10, 16-19, 26, 28-29, 34-38], and oxygenates including carboxylic acids, aldehydes, ketones, fatty alcohols, and esters [4, 6-8, 10, 16-17, 26, 28, 34-38].

The organic liquid products obtained by catalytic cracking of lipid base raw materials including palm oil [10, 16-17], *Mesua ferrea*, L oil [40], residual sunflower oil [19], carboxylic acids [28], animal fats [28], soaps of carboxylic acids [35], as well as the synthetic carboxylic acids derivatives methyl octanoate [41], using sodium salts as basic catalysts (e.g. Na_2CO_3), as well as catalysts with basic properties such as X zeolites (e.g. KNaX1, CsNaX1) produced from FAU zeolites, SBA-15 ordered mesoporous silicate, and clays (sepiolite and hydrotalcite) impregnated with cesium [41], present low concentration of carboxylic acids [10, 16-17, 28, 35, 40-41], due to the catalyst activity in the secondary cracking step, whereas the carboxylic acids are broken up to produce hydrocarbons [2, 42]. The organic liquid products can be refined and/or upgraded by applying physical processes (filtration, decantation, and centrifugation) [10, 16-17, 35-38], and thermal separation processes including distillation [10, 16-17, 28, 35-38, 44-46], liquid-liquid extraction [43-44], and adsorption [44], to produce high quality green fuel-like fractions with potential to substitute partially fossil fuels. The disadvantages of organic liquid products obtained by catalytic cracking of lipid base raw materials including of vegetable oils, residual oils, animal fats, mixture of carboxylic acids, scum, grease, and fats, soaps of carboxylic acids, and residual animal fats remains on the high acid values, if catalysts with acid properties and/or characteristics are used [6-7, 11-13, 15, 18, 21, 23-24, 30-33, 36-38], as well as the high concentrations of olefins, making it a corrosive and unstable fuel [1, 10].

In the last years, thermal separation processes have been applied to remove and/or recover the oxygenates compounds from organic liquid products, particularly fractionation by using single stage and multistage distillation to obtain hydrocarbons-like fuels in the temperature boiling point range of gasoline, kerosene, and diesel-like fractions [6-7, 10, 12, 14, 16-17, 18-19, 22-23, 26, 28, 35-38, 44-46], as well as oxygenates from biomass-derived bio-oils by applying separation and purification processes including molecular distillation [47-51], fractional distillation [52-57], liquid-liquid extraction [43-44, 58-59]. However, until the moment no systematic study has been reported in the literature related to the simulation of organic liquid products (OLP) fractionation and/or purification in multistage countercurrent absorber/stripping columns using supercritical CO_2 as solvent using the chemical process simulator Aspen-HYSYS.

Multistage gas extraction in countercurrent columns has been considered as an alternative separation technique for the extraction and fractionation of liquid mixtures with potential applications in the food industry [60-62]. The applications include removal of terpenes from citrus oils [63-72], separation of fatty acids ethyl esters from butteroil, fish oil, and model mixtures [73-75], isolating of polycyclic aromatic hydrocarbon (PAH) oligomers [76], Isolation of antioxidant compounds from orange juice [77-78], deacidification of olive and rice bran oils [79-82], fractionation of fatty acids from palm fatty acid distillates [83-84], purification of fat-soluble substances (tocopherols, sterols, carotenes, and squalene) from palm oil, olive oil, soya deodorize distillates, olive oil deodorize distillates,

and hexane extract of olive leaves [81, 85-90], fractionation of alcoholic beverages to obtain distillates with lower alcoholic content [91-92], separation of ethanol from aqueous solutions [93], separation of aroma constituents from aqueous solutions of apple, brandy, and wine-must aroma [94-96], fractionation of non-esterified alkoxyglycerols from shark liver oil [97], and fractionation of the model mixture squalene/methyl oleate [98-101].

Despite the wide range of application of multistage gas extraction in countercurrent packed columns, particularly in the food industry, as reported on the reviews by Brunner and Bejarano *et. al.* [62, 102], only a few numbers of works are devoted to simulation of multistage gas extraction using self-made computer codes or commercial chemical process simulators such as Aspen-HYSYS, as described chronologically as follows [103-112]:

Moricet [103], in a pioneer computer simulation study in the early of the 1980s, developed a self-made computer code in Fortran to simulate the separation of mono-glycerides from a model mixture of oleic acid/glycerides as well as the separation of fatty acids from palm oil in countercurrent columns using carbon dioxide as solvent.

Simões and Brunner [104], applied high pressure phase equilibrium data of the system olive oil/CO₂ to simulate a countercurrent packed column for the deacidification of olive oil, by using a staged-equilibrium model self-made program, and the simulations compared with experimental mass transfer data.

Mendes *et. al.* [105], studied the concentration of tocopherols from soybean oil deodorizer distillate, represented as a synthetic mixture of tocopherol/squalene/carboxylic acids, by simulating the separation of tocopherol from a synthetic mixture of tocopherol/squalene/carboxylic acids using SC-CO₂ as solvent within a flowsheet consisting of a one stage extractor and a flash separator using the commercial simulator ASPEN+. The PR-EOS with the LCVM mixing rule thermodynamic fluid package used to correlate the equilibrium data of the system soybean oil deodorizer distillate/CO₂ [106].

Benvenuti *et. al.* [107], used experimental data for a semi-continuous single-stage extractor to remove the terpenes from lemon essential oil using SC-CO₂ as solvent to model the process by assuming equilibrium between the coexisting gaseous phase at the exit of single-stage apparatus and the liquid phase inside it, being the equilibrium described by the PR-EOS, using a self-made academic computer. The thermodynamic modeling of the system extended to study the steady state simulation of a multistage column with solvent recycle of the solvent, represented by a flowsheet consisting of a series of flash separators using the PR-EOS with quadratic mixing rules as thermodynamic fluid package.

Moraes *et. al.* [108], simulated the recovery of provitamin A from esterified palm oil using a mixture of SC-CO₂/ethanol as solvent with the commercial simulator HYSYSTM, by adapting the process units to typical operating conditions of SFE. Because esterified palm oil is a complex mixture, it was necessary to insert the compounds as hypothetical to predict/estimate the physical and thermos-physical properties using the UNIFAC group contribution. The optimization performed for each unit of process based on state conditions (T, P) to obtain a maximum carotenes recovery. The carotenes concentrated with high yields using 02 SFE cycles, and the ethyl esters as by products.

Vásquez *et. al.* [85], applied the GC-EOS to simulate the separation process and for the design of experimental conditions. The thermodynamic model used to obtain optimal process conditions to enhance squalene recovery, including reflux of extracts and recirculation of SC-CO₂ in a continuous countercurrent extraction column.

Fernandes *et. al.* [100], developed a dynamic model of SFE process applied to the fractionation of a binary mixture squalene/methyl oleate by SC-CO₂. The flowsheet, modularly organized into a set of sub-models, includes a countercurrent packed column, a separator, a heat exchanger, and the make-up of CO₂, showing good agreement between experimental and predicted results. The model correctly predicts the outlet streams composition profiles of all the case studies.

Fernandes *et. al.* [101], developed a non-isothermal dynamic model to simulate the fractionation of a binary mixture squalene/methyl oleate with SC-CO₂ in a countercurrent column with structured packing. The model solves the momentum and energy balances within the packed column. The coexisting liquid-gaseous phases assumed to be in local

thermal equilibrium, showing good agreement between measured and predicted temperature and composition profiles of gas and liquid phases along with the column. The model also applied to determine optimal extraction conditions that maximize squalene recovery.

Fornari *et al.* [81], applied the GC-EOS to simulate the deacidification of olive oil and the recovery of minor lipid compounds in a countercurrent packed column using SC-CO₂. The GC-EOS model used to represent phase equilibria of the multicomponent system oil/CO₂, as well as to simulate and optimize the SFE process.

Vásquez *et al.* [82], applied the GC-EOS to simulate the deacidification of olive oil in a countercurrent column using SC-CO₂. The olive oil represented by a binary model mixture oleic acid/triolein, showing a satisfactory agreement between the experimental and computed yields, as well as carboxylic acids content in raffinates.

da Silva [109], simulated the fractionation of liquid mixtures, including the deacidification of olive oil and enriching of fat-soluble substances from soya **deodorize distillates**, in countercurrent column using SC-CO₂ with the chemical process simulator Aspen-HYSYS.

Fernandes *et al.* [110], developed a complete non-isothermal dynamic model to simulate a SFE plant. The flowsheet modularly organized into a set of sub-models of the main unit operations, including the countercurrent packed column operating with reflux, a compressor, a heat exchanger, a separator, and the CO₂ make-up. The modules interconnected by appropriate boundary conditions that couple the mass, momentum, and energy equations. The model showed good agreement between experimental and predicted results.

Pieck *et al.* [111], simulated the extract and raffinate compositions and gas loadings by the fractionation of water/ethanol mixtures in countercurrent columns using SC-CO₂ as solvent, in laboratory, pilot, and industrial scales, by applying thermodynamic, mass transfer, and hydrodynamics models, as well as an equilibrium-stage model. The main objective was proposed contribute a sizing methodology for countercurrent column using SC-CO₂ as solvent.

Costa *et al.* [112], simulate the SC-CO₂ fractionation of organic liquid product (OLP), obtained by catalytic cracking of palm oil at 450 °C, 1.0 atm, using 10% (wt.) Na₂CO₃ as catalyst. The simulations were performed by selecting the multistage countercurrent absorber/stripping unit operation column using SC-CO₂ as solvent with aid the chemical process simulator Aspen-HYSYS 8.6 (Aspen One, 2015) at 333 K and 140 bar, 333 K and 180 bar, and solvent-to-feed ratios (S/F) = 12, 15, 17, 25, 30, 38, applying flowsheets with 01 absorber column and 02 absorber columns. The best deacidifying condition obtained at 333 K, 140 bar, and (S/F) = 17, presenting a top stream yield of 36.65% with 96.95% (wt.) hydrocarbons and 3.05% (wt.) oxygenates, showing a decrease on the oxygenates content in OLP feed from 10% (wt.), with 2.63% (wt.) carboxylic acids, to 3.05% (wt.) oxygenates, with 0.52% (wt.) carboxylic acids.

The objective of this work was to apply the chemical process simulator Aspen-HYSYS 8.6 (Aspen One, 2015) to simulate the SC-CO₂ deoxygenation/deacidification of organic liquid product (OLP), obtained by catalytic cracking of palm oil at 450 °C, 1.0 atm, using 10% (wt.) Na₂CO₃ as catalyst [17]. The simulations were performed by selecting the multistage countercurrent absorber/stripping unit operation column. A new flowsheet was addressed consisting of 03 absorber columns, 10 expansions valves, 10 flash drums, 08 heat exchanges, 01 pressure pump, and 02 make-up of CO₂, aiming to improve the deacidification of OLP. The simulation was performed at 333 K, 140 bar, and (S/F) = 17; 350 K, 140 bar, and (S/F) = 38; 333 K, 140 bar, and (S/F) = 25. The process performance was evaluated by analyzing the yield, recovery of hydrocarbons, olefins, oxygenates, carboxylic acids in the top and bottom streams, as well as the feasibility to obtain deacidify OLP fractions with lower content of alkenes (olefins).

2. Methodology

2.1. Simulation methodology

The organic liquid products (OLP) obtained by thermal catalytic cracking of palm oil at 450 °C, 1.0 atm, using 10% (wt.) Na_2CO_3 as catalyst, in pilot scale, is a complex mixture of hydrocarbons (alkanes, alkenes, cycloalkanes, and aromatics) and oxygenates (carboxylic acids, ketones, and alcohols) [17]. Since high pressure phase equilibrium data for the binary pairs OLP-compounds-i/ CO_2 are scarce, the chemical composition of OLP determined by GC-MS identified approximately 90% (area.) hydrocarbons and 10% (area.) oxygenates, and that acidity is mainly due to the presence of carboxylic acids, OLP has been described by the key-compounds hydrocarbons (*Decane*, *Undecane*, *Tetradecane*, *Pentadecane*, *Hexadecane*, and *Octadecane*) and oxygenates (*Palmitic acid*, *Oleic acid*) [112-113]. The simulations performed by selecting the unit operation multistage countercurrent absorber, as the dissolution/solubilization of gases (CO_2) in liquids (OLP) is a function of state conditions (P , T), and that a fraction of the coexisting liquid phase dissolves in the gas phase, like a gas (CO_2)-liquid (OLP) equilibrium behavior. In the multistage countercurrent absorber column, the fraction collected at the top stream is the extract, that is, a phase rich in SC-CO_2 , containing the more soluble compounds, in this case, the hydrocarbons (*Decane*, *Undecane*, *Tetradecane*, *Pentadecane*, *Hexadecane*, and *Octadecane*), while the fraction collected at the bottom stream is the raffinate, that is, a phase rich in OLP or CO_2 , containing the less soluble compounds, in this case, the oxygenates (*Palmitic acid*, *Oleic acid*).

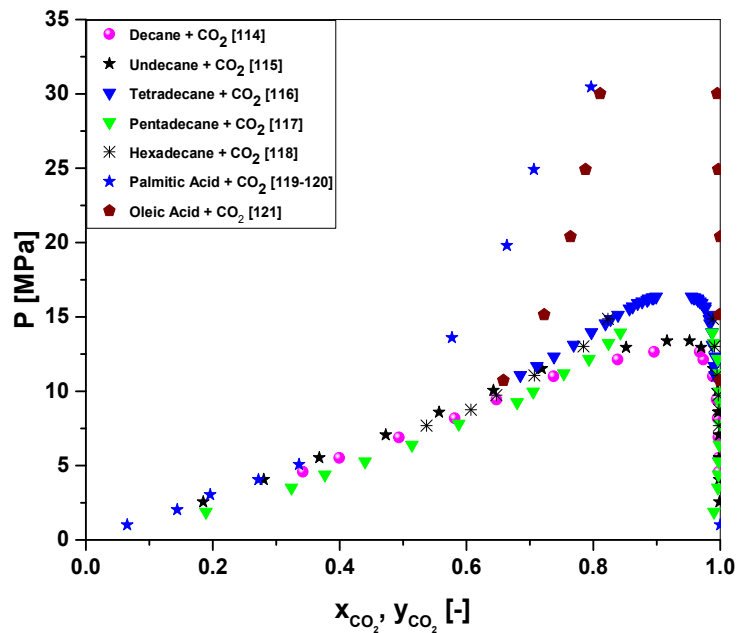


Figure 1. High pressure phase equilibrium for the binary pairs OLP-compounds-i + CO_2 (*Decane* + CO_2 , *Undecane* + CO_2 , *Tetradecane* + CO_2 , *Pentadecane* + CO_2 , *Hexadecane* + CO_2 , *Palmitic acid* + CO_2 , and *Oleic acid* + CO_2) described in the literature [114-121].

The P - x_{CO_2} - y_{CO_2} for the high pressure phase equilibrium data for the binary pairs OLP-compounds-i + CO_2 (*Decane* + CO_2 , *Undecane* + CO_2 , *Tetradecane* + CO_2 , *Pentadecane* + CO_2 , *Hexadecane* + CO_2 , *Palmitic acid* + CO_2 , and *Oleic acid* + CO_2) shows that phase envelop of all the binary pairs hydrocarbons-i + CO_2 (*Decane* + CO_2 , *Undecane* + CO_2 , *Tetradecane* + CO_2 , *Pentadecane* + CO_2 , *Hexadecane* + CO_2) closes between 12.654 and 16.354 MPa and the phase envelope of binary pairs hydrocarbons-i + CO_2 limits the separation of hydrocarbons and

carboxylic acids (oxygenates). In this context, the simulation should be performed between 12.654 and 16.354 MPa. In fact, the state conditions (P, T) to be chosen should take into account not only the solubility of OLP in the SC-CO₂, a physicochemical property associated to the solvent-to-feed ratio (S/F), but also the fraction of carboxylic acids into OLP dissolved in SC-CO₂ (selectivity). The higher the solubility of OLP in the SC-CO₂, the lower the solvent-to-feed ratio (S/F), but lower the selectivity. On the other hand, the lower the solubility of OLP in the SC-CO₂, the higher the solvent-to-feed ratio (S/F), but higher the selectivity. Therefore, a compromise must be found between the solubility of OLP in the SC-CO₂ and the selectivity of OLP compounds in SC-CO₂, there is, between the solvent-to-feed ratio (S/F) and the fraction of carboxylic acids into OLP dissolved in SC-CO₂, as the deoxygenation aims to obtain extracts, there is, OLP containing very low concentrations carboxylic acids and raffinates with high concentrations of carboxylic acids. Based on the analysis of high pressure phase equilibrium data for the binary pairs OLP-compounds-i + CO₂, the state conditions chosen was P = 14.0 MPa and 333 K ≤ T ≤ 350 K.

The OLP deoxygenation process, using SC-CO₂ as solvent, was simulated using Aspen-HYSYS 8.6 (Aspen One, 2015). The simulations performed by selecting the multistage countercurrent absorber/stripping unit operation because of its similarities and/or theoretical thermodynamic fundamentals of solubility of gas in liquids, as the phase equilibrium behaves like a gas-liquid coexisting phases, as described elsewhere [112-113]. Aspen-HYSYS 8.6 computes the countercurrent multistage absorber column unit operations by applying the inside-out algorithm to solve simultaneously materials and energies balances stage-to-stage coupled with a rigorous thermodynamic model. The RK-Aspen EOS with the adjusted binary interaction parameters was selected as fluid package to compute the mixture properties for the multicomponent mixture OLP/SC-CO₂ [112-113].

Organic liquid products obtained by thermal catalytic cracking of palm oil at 450 °C, 1.0 atmosphere, with 10% (wt.) Na₂CO₃ as catalyst, containing 89.24% (area.) hydrocarbons and 10% (area.) oxygenates was used as feed stream [17, 112]. The operating conditions by simulation of OLP deoxygenation process, using SC-CO₂ as solvent, with aid the chemical process simulator Aspen-HYSYS 8.6 (Aspen One, 2015) are described in Table 1.

Operating conditions	
Absorber Column 1	T = 333 K
Feed = 100 kg/h	P = 140 bar
Numbers of stages = 10	(S/F) = 17
Absorber Column 2	T = 350 K
Numbers of stages = 10	P = 140 bar
Feed = Raffinate 1	(S/F) = 38
Absorber Column 3	T = 333 K
Numbers of stages = 10	P = 140 bar
Feed = Raffinate 2	(S/F) = 25

Table 1. Operating conditions by simulation of OLP deoxygenation process, using SC-CO₂ as solvent, with aid the chemical process simulator Aspen-HYSYS 8.6 (Aspen One, 2015).

The process performance was evaluated based on yields of hydrocarbons and oxygenates, as well as the recovery of hydrocarbons, olefins, oxygenates and carboxylic acid in OLP fractions process streams. The yield and recovery of process stream i are computed as follows:

$$Yield_i[\%] = \frac{m_i}{m_{OLP}} \quad (1)$$

$$\text{Recovery}_j[\%] = \frac{\omega_j \cdot \dot{m}_i}{\omega_{j,OLP} \cdot \dot{m}_{OLP}} \quad (2)$$

Where \dot{m}_i and \dot{m}_{OLP} are the mass flow rates of process stream i and OLP feed stream, and ω_j and $\omega_{j,OLP}$ the mass fractions of hydrocarbons or oxygenates chemical functions of process stream i and OLP feed stream.

2.2. Simulation methodology and procedures

The Aspen-HYSYS chemical process simulator uses, for all separation processes and procedures, rigorous calculation for the mass and energy balances, providing a strong basis for simulations inclosing unit operations, thermodynamics, and chemical reactors. The software has a huge flexibility and can simulate different chemical processes according to the user's assembly [112].

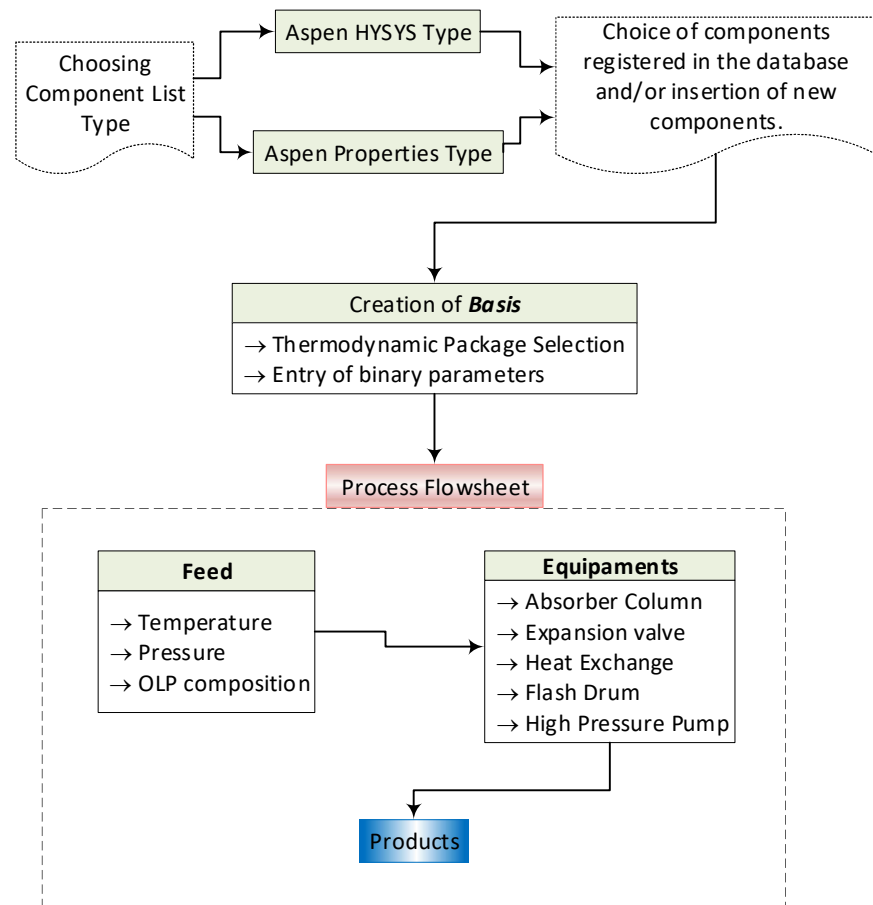


Figure 2. Process simulations steps using Aspen-HYSYS 8.4 by deacidification/deoxygenation of OLP, as described elsewhere [112]: 1-Selection of component list type; 2-Formulation of the list of components; 3-Basis formulation; 4-Flowsheet assembly of the process.

In this work, the Aspen-HYSYS was applied to perform simulations aiming to deacidify OLP in a multistage absorber column, in countercurrent mode, using SC-CO₂ as a solvent. In general, process simulations using Aspen-HYSYS 8.4 consist of in the following steps [112]: 1-Selection of component list type; 2-Formulation of the list of components; 3-Basis formulation; 4-Flowsheet assembly of the process, as shown in Figure 2.

2.3. Simulation process flowsheet strategy

In a previous work, Costa *et. al.* [113] provided the thermodynamic data basis and the EOS modeling to simulate the deoxygenation of OLP obtained by thermal-catalytic cracking of palm oil at 450 °C, 1.0 atm, with 10% (wt.) Na₂CO₃ [17], making it possible to perform the process simulation of OLP deoxygenation by multistage countercurrent absorber with SC-CO₂ as solvent using the process simulator Aspen-HYSYS. Costa *et. al.* [112], simulated the fractionation of OLP obtained by thermal catalytic cracking of palm oil at 450 °C, 1.0 atm, with 10% (wt.) Na₂CO₃ in countercurrent multistage absorber columns using CO₂ as solvent with Aspen-HYSYS, proposing flowsheets with 01 (one) absorber column (flowsheet I) and 02 (two) absorber columns (flowsheet II), where the bottom stream of first absorber column was used as feed in a second absorber column using SC-CO₂ as solvent, as described in details in the literature [112]. *This work address a new flowsheet, consisting of 03 (three) absorber columns, aiming to improve the deacidification of organic liquid products.*

The algorithm, shown in sub-flowsheets I and II illustrated in Figures 3 and 4, respectively, describes in details the procedures necessary to perform the simulation of OLP deacidification/deoxygenation, obtained by thermal catalytic cracking of palm oil at 450 °C, 1.0 atm, and 10% (wt.) Na₂CO₃ as catalyst, in multistage countercurrent absorber columns using SC-CO₂ as solvent. Initially, OLP enters at the top of absorber-01 and SC-CO₂ at the bottom in countercurrent mode. After equilibrium is achieved at a particular state condition (T₁, P₁), 02 (two) coexisting phases, a dense gaseous, rich in SC-CO₂, containing the high soluble/dissolved compounds (hydrocarbons) of OLP, and a liquid, poor in OLP, containing large amounts of dissolved CO₂. The dense gaseous phase exits the top of absorber-01, while the liquid phase exits the bottom of absorber-01. In order to remove CO₂ in the top stream it is necessary not only perform a state transition from SC-CO₂→G-CO₂, but also guarantee that light OLP compounds are no longer dissolved in G-CO₂. In this context, it is necessary to change the state conditions by adding a expansion valve followed by a heat exchanger to remove or add thermal energy, if necessary, to bring the temperature close to ambient conditions, as well as a flash drum to separate subcritical gaseous CO₂ and/or gaseous CO₂ from OLP. If the state conditions of OLP that leaves the bottom of flash drum still permits dissolved CO₂ to co-exist in OLP, then, it is necessary to add an expansion valve to bring the pressure close to ambient condition followed by a heat exchanger to add thermal energy, if necessary, to bring the temperature close to ambient conditions (T = 298 K), as well as a flash drum to separate gaseous CO₂ from OLP. If all the gaseous CO₂ is released at the top of flash drum by ambient conditions (T ≈ 298 K, P ≈ 1.0 bar) and the OLP that leaves the bottom of flash drum contains no longer dissolved CO₂, the separation step is completed.

The liquid that exits the bottom of absorber-01, poor in OLP, containing large amounts of dissolved CO₂, enriched by the low soluble/dissolved compounds (oxygenates) of OLP enters at the top of absorber-02 as feed, while fresh SC-CO₂ (make-up) enters at the bottom of absorber-02 at the same state condition of liquid stream (T₂, P₁). After equilibrium is achieved (T₂, P₁), 02 (two) coexisting phases, a dense gaseous, rich in SC-CO₂, containing the high soluble/dissolved compounds (hydrocarbons) of OLP, and a liquid, poor in OLP, containing large amounts of dissolved CO₂. The dense gaseous phase exits the top of absorber-02, while the liquid phase exits the bottom of absorber-02. In order to remove CO₂ in the top stream it is necessary not only perform a state transition from SC-CO₂→G-CO₂, but also guarantee that light OLP compounds are no longer dissolved in G-CO₂. Adding an expansion valve makes it possible to change the state conditions, as well as a heat exchanger to remove or add thermal energy, *if necessary*, to bring the temperature close to ambient conditions. Afterwards, a flash drum is added to separate the subcritical gaseous CO₂ and/or gaseous CO₂ from OLP. If the OLP that leaves the bottom of flash drum still contains dissolved CO₂, then, an expansion valve is added to bring the pressure close to ambient condition followed by a heat exchanger to supply thermal energy, *if necessary*, to bring the temperature close to ambient conditions (T = 298 K), as well as a flash drum to separate gaseous CO₂ from OLP. If all the gaseous CO₂ is released

at the top of flash drum by ambient conditions ($T \approx 298$ K, $P \approx 1.0$ bar) and the OLP that leaves the bottom of flash drum contains no longer dissolved CO_2 , the separation step is completed.

The liquid phase leaving the bottom of absorber-02, poor in OLP, contains large amounts of dissolved CO_2 that must be removed and separate from OLP. In order to remove CO_2 in the bottom stream it is necessary to change the state conditions to diminish the solubility of CO_2 in OLP. Adding an expansion valve makes it possible to change the state conditions of soluble/dissolved CO_2 from liquid to subcritical gaseous CO_2 and/or gaseous CO_2 ($\text{L-CO}_2 \rightarrow \text{SC-CO}_2/\text{G-CO}_2$). Afterwards, a flash drum is added to separate the subcritical gaseous CO_2 and/or gaseous CO_2 from OLP. If the OLP that leaves the bottom of flash drum still contains dissolved CO_2 , then, an expansion valve is added to bring the pressure close to ambient condition followed by a heat exchanger to supply thermal energy, *if necessary*, to bring the temperature close to ambient conditions ($T = 298$ K), as well as a flash drum to separate gaseous CO_2 from OLP. If all the gaseous CO_2 is released at the top of flash drum by ambient conditions ($T \approx 298$ K, $P \approx 1.0$ bar) but considerable amounts of OLP still leaves the bottom of flash drum, even though it contains no longer dissolved CO_2 , another absorber should be added to the flowsheet. In order to bring the OLP to the state conditions (T_1, P_1) of absorber-03, a high pressure pump is added after the flash drum bottom stream followed by a heat exchanger to supply thermal energy. The OLP enters at the top of absorber-03 as feed, while fresh SC-CO_2 (make-up) enters at the bottom of absorber-03 at the same state condition of liquid stream (T_1, P_1). After equilibrium is achieved (T_1, P_1), 02 (two) coexisting phases, a dense gaseous, rich in SC-CO_2 , containing the high soluble/dissolved compounds (hydrocarbons) of OLP, and a liquid, poor in OLP, containing large amounts of dissolved CO_2 . The dense gaseous phase exits the top of absorber-03, while the liquid phase exits the bottom of absorber-03. In order to remove CO_2 in the top stream it is necessary not only perform a state transition from $\text{SC-CO}_2 \rightarrow \text{G-CO}_2$, but also guarantee that light OLP compounds are no longer dissolved in G-CO_2 . Adding an expansion valve makes it possible to change the state conditions, as well as a heat exchanger to remove or add thermal energy, *if necessary*, to bring the temperature close to ambient conditions. Afterwards, a flash drum is added to separate the gaseous CO_2 from OLP. If the OLP that leaves the bottom of flash drum still contains dissolved CO_2 , then, an expansion valve is added to bring the pressure close to ambient condition followed by a heat exchanger to supply thermal energy, *if necessary*, to bring the temperature close to ambient conditions ($T = 298$ K), as well as a flash drum to separate gaseous CO_2 from OLP. If all the gaseous CO_2 is released at the top of flash drum by ambient conditions ($T \approx 298$ K, $P \approx 1.0$ bar) and the OLP that leaves the bottom of flash drum contains no longer dissolved CO_2 , the separation step is completed.

The liquid phase leaving the bottom of absorber-03, poor in OLP, contains large amounts of dissolved CO_2 that must be removed and separate from OLP. In order to remove CO_2 in the bottom stream it is necessary to change the state conditions to diminish the solubility of CO_2 in OLP. Adding an expansion valve makes it possible to change the state conditions of soluble/dissolved CO_2 from liquid to gaseous CO_2 ($\text{L-CO}_2 \rightarrow \text{G-CO}_2$). Afterwards, a flash drum is added to separate the gaseous CO_2 from OLP. If the OLP that leaves the bottom of flash drum still contains dissolved CO_2 , then, an expansion valve is added to bring the pressure close to $P \approx 1.0$ bar followed by a heat exchanger to supply thermal energy, *if necessary*, to bring the temperature close to $T \approx 298$ K, as well as a flash drum to separate gaseous CO_2 from OLP. If all the gaseous CO_2 is released at the top of flash drum by ambient conditions ($T \approx 298$ K, $P \approx 1.0$ bar) and the OLP that leaves the bottom of flash drum contains no longer dissolved CO_2 , the separation step is completed.

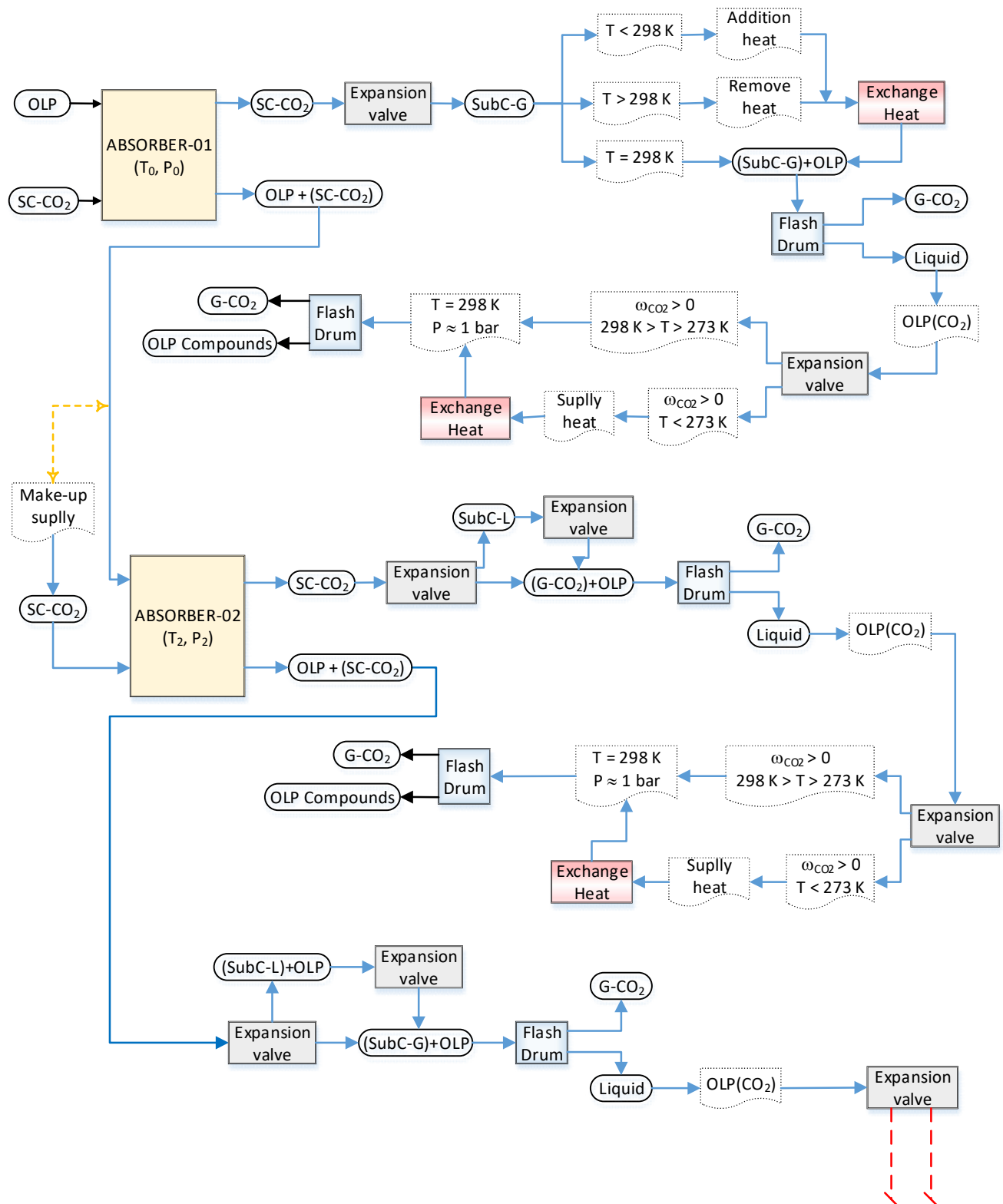


Figure 3. Flowsheet algorithm simulation strategy by deacidification/deoxygenation of organic liquid products, obtained by thermal catalytic cracking of palm oil at 450 °C, 1.0 atm, and 10% (wt.) Na₂CO₃ as catalyst, in multistage counter-current absorber columns using SC-CO₂ as solvent, illustrating sub-flowsheet I with absorbers 01 and 02.

3. Results and discussions

3.1. Process simulation

3.1.1. Process flowsheet

The proposed flowsheet illustrated in Figure 5 consists of 03 absorber columns, 10 expansion valves, 10 flash drums, 08 heat exchangers, 01 high pressure pump, and 02 make-ups of CO₂, aiming to optimize the deacidification of organic liquid products.

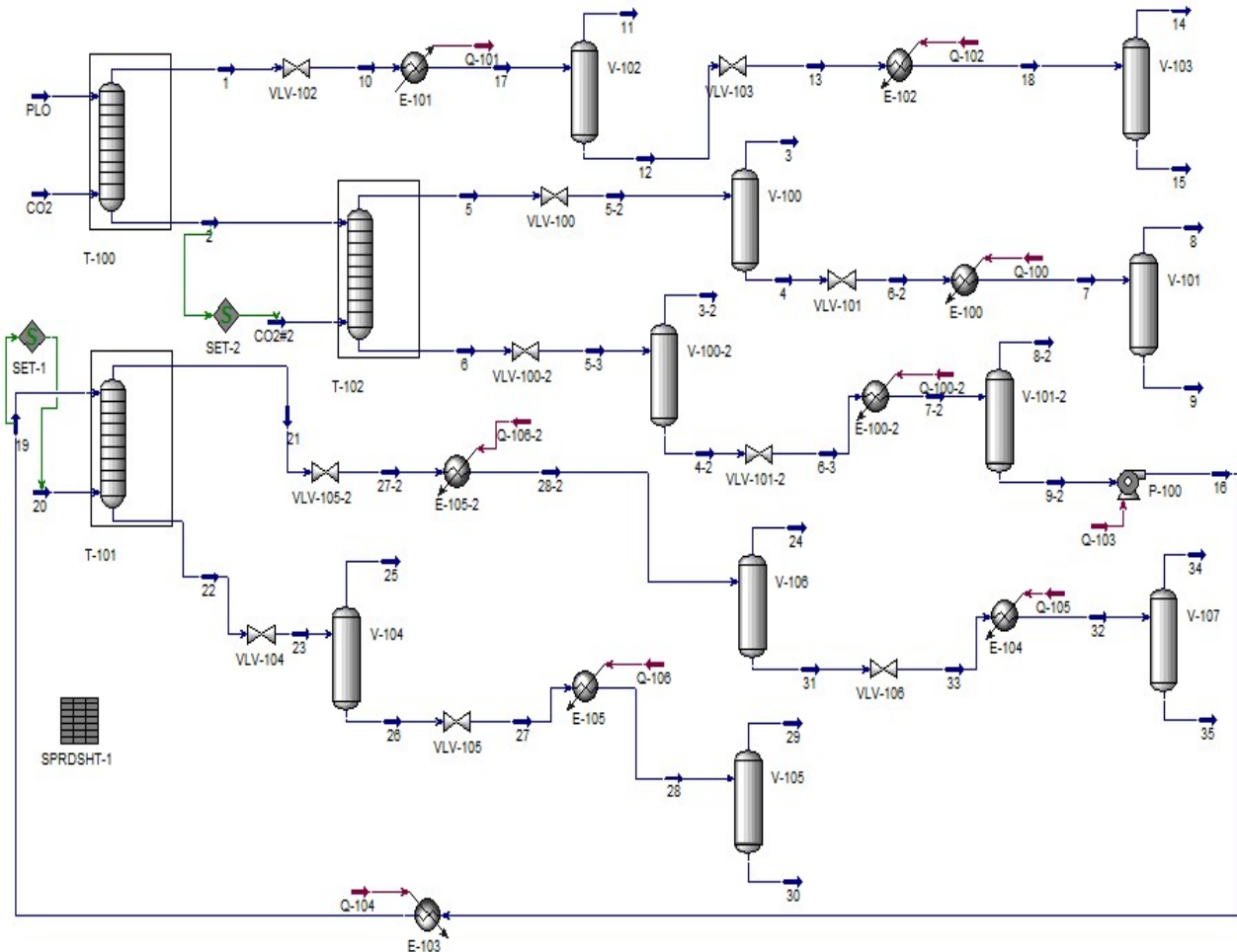


Figure 5. Process flowsheet [absorber columns (T-100, T-101, T-102); flash drums (V-100, V-100-2, V-101, V-101-2, V-102, V-103, V-104, V-105, V-106, V-107); valves (VLV-100, VLV-100-2, VLV-101, VLV-101-2, VLV-102, VLV-103, VLV-104, VLV-105, VLV-105-2, VLV-106); heat exchangers (E-100, E-100-2, E-101, E-102, E-103, E-104, E-105, E-105-2), make-ups (SET-1, SET-2), high pressure pump (P-100)] by OLP deoxygenation in multistage countercurrent absorber columns using CO₂ as solvent (Raffinate 1 + CO₂ as feed top stream of absorber T-102, Raffinate 2 as feed top stream of absorber T-101, and CO₂ make up as feed bottom stream of absorber T-102 and of absorber T-101).

Table 2 shows the material (molar and mass flow rates) and energy balances (heat flow rates), fractions of gas phase, as well as the state conditions (T, P) for all the process streams by simulation of OLP deoxygenation process in multistage countercurrent absorber columns using CO₂ as solvent, using Aspen-HYSYS 8.6 (Aspen One, 2015), expressed in CO₂ basis, at 333 K, 140 bar, and (S/F) = 17; at 350 K, 140 bar, and (S/F) = 25; and at 333 K, 140 bar, and (S/F) = 38.

Stream N ^o	$\omega_{i, Gas}$	T [°C]	P [bar]	Molar Flow [kmol/h]	Mass Flow [kg/h]	Liquid Vol. Flow [m ³ /h]	Heat Flow [kcal/h]		Heat Flow [kcal/h]
PLO	0	60	140	0.5196	100	0.1214	-43708.4	Q-100	1361.1
CO ₂	1	60	140	38.4232	1691	2.0578	-3672925.4	Q-101	19905.9
1	1	147.94	140	20.0574	910.0584	1.1081	-1872017.7	Q-102	763.3
2	0.92522	77.78	140	18.8854	880.9416	1.0712	-1794358.8	Q-100-2	80.7
5	1	93.54	140	49.8952	2227.474	2.7105	-4718556.9	Q-103	154.0
6	0.93017	98.15	140	5.1121	243.186	0.2952	-483682.8	Q-104	318.3
CO ₂ #2	1	77.78	140	36.1219	1589.718	1.9346	-3431362.5	Q-106	2496.4
3	1	21.64	40	49.1959	2165.239	2.6349	-4652389.5	Q-106-2	1843.5
4	0	21.64	40	0.6993	62.2349	7.56E-02	-66167.4	Q-105	214.0
5-2	0.98598	21.64	40	49.8952	2227.474	2.7105	-4718556.9		
6-2	0.66532	-37.00	1.5	0.6993	62.2349	7.56E-02	-66167.4		
7	0.69432	25	1.5	0.6993	62.2349	7.56E-02	-64806.3		
8	1	25	1.5	0.4855	21.3767	2.60E-02	-45671.2		
9	0	25	1.5	0.213767	40.8581	4.95E-02	-19135.1		
10	0.98826	107.40	45	20.0574	910.0584	1.1081	-1872017.7		
11	1	35	45	19.4630	856.909	1.0428	-1838423.0		
12	0	35	45	0.5943	53.1494	6.53E-02	-53500.6		
13	0.62478	-14.02	1.5	0.5943	53.1494	6.53E-02	-53500.6		
14	1	25	1.5	0.3794	16.7190	2.03E-02	-35684.9		
15	0	25	1.5	0.2149	36.4304	4.49E-02	-17052.4		
17	0.97036	35	45	20.0574	910.0584	1.1081	-1891923.6		
18	0.63841	25	1.5	0.5943	53.1494	6.53E-02	-52737.3		
3-2	1	46.09	50	4.8689	214.2947	0.2607	-459529.9		
4-2	0	46.09	50	0.2432	28.8913	3.45E-02	-24152.8		
5-3	0.95242	46.09	50	5.1121	243.186	0.2952	-483682.8		
6-3	0.57602	18.04	1.5	0.2432	28.8913	3.45E-02	-24152.8		
7-2	0.57774	25	1.5	0.2432	28.8913	3.45E-02	-24072.1		
8-2	1	25	1.5	0.1405	6.1840	7.53E-03	-13217.3		
9-2	0	25	1.5	0.1026	22.7073	2.70E-02	-10854.8		
16	0	30.12	140	0.1026	22.7073	2.70E-02	-10700.7		
19	0	60	140	0.1026	22.7073	2.70E-02	-10382.4		
20	1	60	140	6.1480	270.5742	3.29E-01	-587699.0		
21	1	72.81	140	4.1244	185.1077	2.25E-01	-392745.7		
22	0.99080	60.39	140	2.1263	108.1738	0.1310	-204486.5		
23	0.51057	25.12	60	2.1263	108.1738	0.1310	-204486.5		
25	1	25.12	60	1.085	47.7824	5.81E-02	-103080.1		
29	1	25	1.5	0.9589	42.2025	5.14E-02	-90200.8		
30	0	25	1.5	8.18E-02	18.1888	2.16E-02	-8709.2		
27	0.68209	-82.52	1.5	1.0406	60.3913	7.29E-02	-101406.4		
28	0.92143	25	1.5	1.0406	60.3913	7.29E-02	-98910.0		

26	0	25.12	60	1.0406	60.3913	7.29E-02	-101406.4		
27-2	0.84043	15.85	50	4.1244	185.1077	2.25E-01	-392745.7		
28-2	0.97521	25	50	4.1244	185.1077	2.25E-01	-390902.2		
24	1	25	50	4.0221	177.0208	2.15E-01	-380896.7		
31	0	25	50	0.1022	8.0869	9.73E-03	-10005.5		
32	0.79566	25	1.5	0.1022	8.0869	9.73E-03	-9791.4		
34	1	25	1.5	8.13E-02	3.5796	4.36E-03	-7650.9		
35	0	25	1.5	2.09E-02	4.5072	5.37E-03	-2140.5		
33	0.74861	-54.91	1.5	0.1022	8.0869	9.73E-03	-10005.5		

Table 2: Material and energy balances and state conditions (T, P) for all the process streams by simulation of OLP deoxygenation process in multistage countercurrent absorber columns using CO₂ as solvent, using Aspen-HYSYS 8.6 (Aspen One, 2015), expressed in CO₂ basis, at 333 K, 140 bar, and (S/F) = 17; at 350 K, 140 bar, and (S/F) = 25; and at 333 K, 140 bar, and (S/F) = 38.

In addition, supplementary Tables S1, S2, and S2 provide detailed information of process conditions, mass flow rates, gaseous fractions, recoveries of hydrocarbons and oxygenates in extract and raffinate, as well as chemical composition, expressed in solvent-free basis, of hydrocarbons and oxygenates of OLP in feed, top and bottom streams of absorber columns T-100, T-102, and T-101 by simulation of OLP deoxygenation process in multistage countercurrent absorber columns using CO₂ as solvent, using Aspen-HYSYS 8.6 (Aspen One, 2015) at 333 K, 140 bar, and (S/F) = 17; at 350 K, 140 bar, and (S/F) = 25; and at 333 K, 140 bar, and (S/F) = 38.

The stream 1 leaving the top of absorber column T-100, rich in carbon dioxide the supercritical state, with a gaseous phase solubility $y_{CO_2, OLP} = 0.9597$, very close to $y_{CO_2, n\text{-undecane}} = 0.9518$ at 344.5 K and 13.4 MPa for the high pressure phase equilibria of binary system n-undecane + CO₂ [115], flows through the expansion valve (VLV-102), causing not only a decrease in pressure and temperature, but also a phase change from supercritical to sub-critical gaseous state, making it possible to separate CO₂ in the gaseous state from organic liquid products. However, if the solubilities of dissolved OLP compounds in gaseous CO₂ is still low but not zero, due to high temperatures at the exit of expansion valve, a heat exchanger (E-101) is placed after the expansion valve to diminish the temperature, thus making it possible the complete separation of gaseous CO₂ and the dissolved OLP compounds within the flash drum (V-102), since the solubilities of dissolved OLP in CO₂ tends to zero. The bottom stream of flash drum (V-102), rich in OLP compounds, still contains dissolved CO₂, thus making it necessary to insert another the expansion valve (VLV-103) at the exit of flash drum (V-102), causing a decrease in pressure and temperature. However, if the temperature is too low that may solidify the condensed OLP compounds, a second heat exchanger (E-102) is placed after the expansion valve to supply thermal energy, in order to increase the temperature, maintaining the OLP compounds in the liquid state, thus making it possible the complete separation of gaseous CO₂ and the condensed OLP compounds within the flash drum (V-103), since the solubilities of dissolved CO₂ into OLP tends to zero.

The OLP at the top stream of absorber column T-100, expressed in solvent-free basis, obtained in bottom stream 15, after separation and/or degassing of gaseous CO₂ in the

flash drums V-102 and V-103, presents on its chemical composition 96.95% (area.) hydrocarbons with 39.14% (area.) of alkanes, 36.39% (area.) of alkenes (olefins) and 21.42% (area.) of naphthene's, as well as 3.05% (area.) oxygenates. By comparing the composition of OLP in stream 15 with that of kerosene-like fraction, containing 93.63% (area.) hydrocarbons (42.62% alkanes, 24.89% alkenes, and 26.12% naphthene's) and 6.37% (area.) oxygenates, obtained by distillation of organic liquid products after thermal catalytic cracking of dehydrated residual fat, oils, and grease (FOG) from grease traps at 450 °C, 1.0 atm, with 10% (wt.) Na₂CO₃, in pilot scale [37], suggests that OLP fraction of the extract in bottom stream 15 of absorber column T-100 resembles the chemical composition of kerosene with lower levels of alkanes and oxygenates. In addition, the recovery of OLP, expressed in solvent-free basis, obtained in bottom stream 15 was 36.65%, as shown in Table 3.

The stream 2 leaving the bottom of absorber column T-100, rich in dissolved CO₂ into OLP, with a liquid phase solubility $x_{\text{CO}_2, \text{OLP}} = 0.9281$, very close to $x_{\text{CO}_2, \text{Undecane}} = 0.9161$ at 344.5 K and 13.4 MPa for the high pressure phase equilibria of binary system n-undecane + CO₂ [115], enters the top of absorber column T-102, as partially acidified hydrocarbons, contains 84.78% (area.) hydrocarbons (43.54% alkanes, 18.95% alkenes, and 22.29% naphthene's) and 15.22% (area.) oxygenates. Fresh CO₂, supplied by a make-up, enters the bottom of absorber column T-102 in order to achieve the solvent-to-feed ratio of (S/F) = 38. The stream 5 leaving the top of absorber column T-102, rich in carbon dioxide in the supercritical state, with a gaseous phase solubility $y_{\text{CO}_2, \text{OLP}} = 0.9817$, very close to $y_{\text{CO}_2, \text{Tetradecane}} = 0.9870$ at 344.5 K and 13.95 MPa for the high pressure phase equilibria of binary system n-undecane + CO₂ [116], flows through the expansion valve (VLV-100), changing the state conditions (T = 294.6 K, P = 40 bar), causing a phase change from supercritical to gaseous state, making it possible to separate CO₂ in the gaseous state from organic liquid products inside flash drum (V-100). The bottom stream of flash drum (V-100), rich in OLP compounds, still contains dissolved CO₂, thus making it necessary to insert another the expansion valve (VLV-101) at the exit of flash drum (V-100), causing a decrease in pressure and temperature (T = 236.0 K, P = 1.5 bar). In cases whereas a drastic decrease on the temperature takes place because of Joule-Thompson effect, that may solidify the OLP compounds, a heat exchanger (E-100) is placed after the expansion valve to supply thermal energy, to bring the temperature to ambient conditions (T = 298 K), thus making it possible the complete separation of gaseous CO₂ and the dissolved OLP compounds within the flash drum (V-101), since the solubilities of dissolved OLP in CO₂ tends to zero.

The OLP at the top stream of absorber column T-102, expressed in solvent-free basis, obtained in bottom stream 9, after separation and/or degassing of gaseous CO₂ in the flash drums V-100 and V-101, contains 92.78% (area.) hydrocarbons (46.53% alkanes, 21.75% alkenes, and 24.49% naphthene's) and 7.22% (area.) oxygenates. By comparing the composition of OLP in stream 9 with that of gasoline-like fraction, containing 92.30% (area.) hydrocarbons (21.52% alkanes, 37.51% alkenes, and 33.27% naphthene's) and 7.70% (area.) oxygenates, obtained by distillation of organic liquid products after thermal catalytic cracking of palm oil at 450 °C, 1.0 atm, with 20% (wt.) Na₂CO₃, in pilot scale [122], suggests that OLP fraction of the extract in bottom stream 9 of absorber column T-102 resembles the

chemical composition of gasoline with lower levels of alkanes and oxygenates. In addition, the recovery of OLP, expressed in solvent-free basis, obtained in bottom stream 9 was 40.77%, as shown in Table 3.

The stream 6 leaving the bottom of absorber column T-102, rich in dissolved CO₂ into OLP, with a liquid phase solubility $x_{\text{CO}_2, \text{OLP}} = 0.9072$, very close to $x_{\text{CO}_2, \text{Undecane}} = 0.9161$ at 344.5 K and 13.4 MPa for the high pressure phase equilibria of binary system n-undecane + CO₂ [115], flows through the expansion valve (VLV-100-2), changing the state conditions, causing a phase change from supercritical (T = 371 K, P = 140 bar) to sub-critical gaseous state (T = 319 K, P = 50 bar), making it possible to separate CO₂ in the gaseous state from organic liquid products inside flash drum (V-100-2). The bottom stream of flash drum (V-100-2), rich in OLP compounds, still contains dissolved CO₂, thus making it necessary to insert another the expansion valve (VLV-101-2) at the exit of flash drum (V-100-2), causing a decrease in pressure (P = 1.5 bar) and temperature (T = 291 K). In order to bring the temperature to ambient conditions, a heat exchanger (E-100-2) is placed after the expansion valve to supply thermal energy, thus making it possible the complete separation of gaseous CO₂ and the dissolved OLP compounds within the flash drum (V-101-2), since the solubilities of dissolved OLP in CO₂ tends to zero. As the stream leaving the bottom of flash drum (V-101-2), still contains large amounts of OLP compounds, a third absorber column is added to the flowsheet to deacidify the OLP compounds. The stream 9-2 is compressed with aid a high pressure pump (P-100) to bring OLP to the state conditions of absorber column T-101 (T = 333 K, P = 140 bar). After the high pressure pump, the state condition of stream 16 is 303 K and 140 bar, thus making it necessary to add a heat exchanger (E-103) to supply thermal energy to bring the temperature to 333 K. The stream 19 (T = 333 K, P = 140 bar) enters the top of absorber column T-101, while fresh CO₂ supplied by make-up (SET-1) enters the bottom of absorber column T-101 at 333 K and 140 bar).

The stream 21 leaving the top of absorber column T-101, rich in CO₂ in the supercritical state, with a gaseous phase solubility $y_{\text{CO}_2, \text{OLP}} = 0.9869$, very close to $y_{\text{CO}_2, \text{Tetradecane}} = 0.9870$ at 344.5 K and 13.95 MPa for the high pressure phase equilibria of binary system n-undecane + CO₂ [116], flows through the expansion valve (VLV-105-2), causing a phase change from supercritical to gaseous state, making it possible to separate CO₂ in the gaseous state from organic liquid products. If the temperature is lower than 298 K, a heat exchanger (E-105-2) is placed after the expansion valve to bring the temperature to 298 K, thus making it possible the separation of gaseous CO₂ and the dissolved OLP compounds within the flash drum (V-106). If the bottom stream of flash drum (V-106), rich in OLP compounds, still contains dissolved CO₂, it is necessary to insert another the expansion valve (VLV-106) at the exit of flash drum (V-106), causing a decrease in pressure and temperature. However, if the temperature is too low that may solidify the condensed OLP compounds, a second heat exchanger (E-104) is placed after the expansion valve (VLV-106) to supply thermal energy, in order to increase the temperature, maintaining the OLP compounds in the liquid state, thus making it possible the complete separation of gaseous

CO₂ and the condensed OLP compounds within the flash drum (V-107), since the solubilities of dissolved CO₂ into OLP tends to zero.

The stream 22 leaving the bottom of absorber column T-101, rich in dissolved CO₂ into OLP, with a liquid phase solubility $x_{\text{CO}_2, \text{OLP}} = 0.9323$, very close to $x_{\text{CO}_2, \text{Undecane}} = 0.9161$ at 344.5 K and 13.4 MPa for the high pressure phase equilibria of binary system n-undecane + CO₂ [115], flows through the expansion valve (VLV-104), causing a phase change from supercritical (T = 333 K, P = 140.0 bar) to gaseous state (T = 298 K, P = 60 bar), making it possible to separate CO₂ in the gaseous state from organic liquid products inside flash drum (V-104). The bottom stream of flash drum (V-104), rich in OLP compounds, still contains dissolved CO₂, thus making it necessary to insert another the expansion valve (VLV-105) at the exit of flash drum (V-104), causing a decrease in pressure (P = 1.5 bar) and temperature (T = 191.0 K). In order to bring the temperature to ambient conditions, a heat exchanger (E-105) is placed after the expansion valve to supply thermal energy, thus making it possible the complete separation of gaseous CO₂ and the dissolved OLP compounds within the flash drum (V-105), since the solubilities of dissolved OLP in CO₂ tends to zero at 298 K and 1.5 bar. The simulated gas-liquid high pressure equilibrium in the exit of absorber columns T-100, T-102, and T-101, given by the $y_{\text{CO}_2, \text{OLP}}$ and $x_{\text{CO}_2, \text{OLP}}$ of streams 1, 2, 3, 6, 21, and 22 are according to high pressure equilibrium data for the binary pairs OLP-compounds-i + CO₂ (*Decane + CO₂*, *Undecane + CO₂*, *Tetradecane + CO₂*, *Pentadecane + CO₂*, *Hexadecane + CO₂*) described in the literature [114-118].

The OLP at the bottom stream of absorber column T-102, expressed in solvent-free basis, obtained in bottom stream 9-2, after separation and/or degassing of gaseous CO₂ in the flash drums V-100-2 and V-101-2, enriched on oxygenates, present on its composition 70.34% (area.) hydrocarbons (38.15% alkanes, 13.88% alkenes, and 18.31% naphthene's) and 29.66% (area.) oxygenates, while the stream 35 at the bottom flash drum (V-107), expressed in solvent-free basis, contains 83.85% (area.) hydrocarbons and 16.15% (area.) oxygenates. The stream 30 at the bottom flash drum (V-105), expressed in solvent-free basis, enriched on oxygenates, contains 67.34% (area.) hydrocarbons and 32.66% (area.) oxygenates. The recovery of OLP, expressed in solvent-free basis, obtained in bottom stream 35 of flash drum (V-107) was 4.07%, as shown in Table 3.

The simulated chemical composition of OLP in stream 15, expressed in CO₂-free basis, shows a yield of 36.65% with 96.95% (wt.) hydrocarbons and 3.05% (wt.) oxygenates. It could be observed a decrease on the oxygenates content in feed OLP from 10% (wt.), with 2.63% (wt.) carboxylic acids, to 3.05% (wt.) oxygenates, with 0.52% (wt.) carboxylic acids [112], showing that the fraction of carboxylic acids in OLP dissolved into SC-CO₂ was very low. This is according to high pressure phase equilibrium data for the binary systems palmitic acid + CO₂ [119-120], and oleic acid + CO₂ [121].

The simulated chemical composition of OLP in stream 9, expressed in CO₂-free basis, shows a yield of 40.77% with 92.78% (wt.) hydrocarbons and 7.22% (wt.) oxygenates. It could be observed a decrease on the oxygenates content in RAF1 from 15.22% (wt.), with 3.85% (wt.) carboxylic acids, to 7.22% (wt.) oxygenates, with 1.47% (wt.) carboxylic acids [112], showing that the fraction of carboxylic acids in OLP dissolved into SC-CO₂ was very low. This is according to high pressure phase equilibrium data for the binary systems palmitic acid + CO₂ [119-120], and oleic acid + CO₂ [121]. Finally, it can be observed in Table

3 that 81.49% (wt.) of feed OLP was recovered in the top streams of absorbers T-100, T-102, and T-101, showing that deacidified OLP with chemical compositions similar to ker- osene-like fraction obtained by distillation of organic liquid products after thermal cata- lytic cracking of dehydrated residual fat, oils, and grease (FOG) from grease traps at 450 °C, 1.0 atm, with 10% (wt.) Na₂CO₃, in pilot scale [37], gasoline-like fraction obtained by distillation of organic liquid products after thermal catalytic cracking of palm oil at 450 °C, 1.0 atm, with 20% (wt.) Na₂CO₃, in pilot scale [122].

	Feed	Column 1		Column 2		Column 3	
(S/F)	-	17		38		25	
	OLP	Top	Botton (RAF1)	Top	Botton (RAF2)	Top	Botton
Mass Flow [kg/h]	100	36.65	63.35	40.77	22.58	4.07	18.49
Mass fraction (CO ₂ free basis)							
Hydrocarbons	0.8924	0.9695	0.8478	0.9278	0.7034	0.8385	0.6734
Alkanes	0.4193	0.3914	0.4354	0.4653	0.3815	0.4321	0.3701
Alkenes	0.2534	0.3639	0.1895	0.2175	0.1388	0.1389	0.1389
Naphthenes	0.2197	0.2142	0.2229	0.2449	0.1831	0.2674	0.1644
Oxygenates	0.1076	0.0305	0.1522	0.0722	0.2966	0.1615	0.3266
Carboxylic acids	0.0263	0.0052	0.0385	0.0147	0.0814	0.0354	0.0916
Alcohols	0.0351	0.0086	0.0505	0.0174	0.1102	0.0412	0.1255
Ketones	0.0462	0.0167	0.0632	0.0402	0.1049	0.0849	0.1094

Table 3: Chemical composition, expressed in solvent-free basis, of hydrocarbons and oxygenates of OLP in feed, top and bottom streams of absorber columns T-100, T-102, and T-101 by simulation of OLP deoxygenation process in multistage countercurrent absorber columns using CO₂ as solvent, using Aspen-HYSYS 8.6 (Aspen One, 2015), expressed in CO₂ basis, at 333 K, 140 bar, and (S/F) = 17; at 350 K, 140 bar, and (S/F) = 25; and at 333 K, 140 bar, and (S/F) = 38.

5. Conclusions

This work address a new flowsheet, consisting of 03 (three) absorber columns, aiming to improve the deacidification of organic liquid products OLP in multistage countercurrent absorber/stripping columns using SC-CO₂ as solvent, with Aspen-Hysys.

The algorithm, shown in sub-flowsheets I and II describes in details the procedures necessary to perform the simulation of OLP deacidification/deoxygenation, obtained by thermal catalytic cracking of palm oil at 450 °C, 1.0 atm, and 10% (wt.) Na₂CO₃ as catalyst, in multistage countercurrent absorber columns using SC-CO₂ as solvent.

The simulation shows that 81.49% of OLP could be recovered and the concentrations of hydrocarbons in the extracts of absorber-01 and absorber-02 were 96.95 and 92.78% (wt.) in solvent-free basis, while the bottom stream of absorber-03 was enriched in oxygenates compounds with concentrations up to 32.66% (wt.) in solvent-free basis, showing that organic liquid products (OLP) was deacidified and SC-CO₂ was able to deacidify OLP and to obtain fractions with lower olefins content.

Supplementary Materials: The following are available online at www.mdpi.com/xxx/s1. **Table S1.** Process conditions, mass flow rates, gaseous fractions, recoveries of hydrocarbons and oxygenates in extract and raffinate, as well as chemical composition, expressed in solvent-free basis, of hydrocarbons and oxygenates of OLP in feed, top and bottom streams of

absorber columns T-100 by simulation of OLP deoxygenation process in multistage countercurrent absorber columns using CO₂ as solvent, using Aspen-HYSYS 8.6 (Aspen One, 2015) at 333 K, 140 bar, and (S/F) = 17. **Table S2.** Process conditions, mass flow rates, gaseous fractions, recoveries of hydrocarbons and oxygenates in extract and raffinate, as well as chemical composition, expressed in solvent-free basis, of hydrocarbons and oxygenates of OLP in feed, top and bottom streams of absorber columns T-102 by simulation of OLP deoxygenation process in multistage countercurrent absorber columns using CO₂ as solvent, using Aspen-HYSYS 8.6 (Aspen One, 2015) at 350 K, 140 bar, and (S/F) = 25. **Table S3.** Process conditions, mass flow rates, gaseous fractions, recoveries of hydrocarbons and oxygenates in extract and raffinate, as well as chemical composition, expressed in solvent-free basis, of hydrocarbons and oxygenates of OLP in feed, top and bottom streams of absorber columns T-101 by simulation of OLP deoxygenation process in multistage countercurrent absorber columns using CO₂ as solvent, using Aspen-HYSYS 8.6 (Aspen One, 2015) at 333 K, 140 bar, and (S/F) = 38.

Author Contributions: The individual contributions of all the co-authors are provided as follows: Manoel Raimundo dos Santos Jr contributed with *formal analysis and writing—original draft preparation*, Elinéia Castro Costa contributed with *formal analysis and writing—original draft preparation*, Marcilene Paiva da Silva contributed with computation of binary interaction parameters with Aspen-HYSYS and simulations, Caio Campus Ferreira contributed with graphics and flowsheets, Lucas Pinto Bernar contributed with graphics and flowsheets, Douglas Alberto Rocha de Castro contributed with *thermal-catalytic cracking experiments*, Marcelo Costa Santos contributed with *thermal-catalytic cracking experiments*, Andréia de Andrade Mâncio contributed with *thermal-catalytic cracking experiments*, Silvio Alex Pereira da Mota contributed with *OLP chemical composition*, Sergio Duvoisin Jr. contributed with *OLP chemical analysis*, Luiz Eduardo Pizarro Borges contributed with *experiments design*, Marilena Emmi Araújo contributed with *supervision, conceptualization, and data curation*, and Nélcio Teixeira Machado contributed with *supervision, conceptualization, and data curation*. All authors have read and agreed to the published version of the manuscript.

Funding: This research was partially funded by CAPES-Brazil.

Acknowledgments: I would like to acknowledge Prof. Dr. Gerd Brunner, former Head of Thermal Separation Process Institute at TUHH, for his marvelous contribution to fractionation of liquid mixtures in countercurrent columns using supercritical carbon dioxide as solvent.

Conflicts of Interest: The authors declare no conflict of interest.

References

1. T. Hua; L. Chunyi; Y. Chaohe, S. Honghong. Alternative processing technology for converting vegetable oil and animal fats to clean fuels and light olefins. *Chinese Journal of Chemical Engineering*. 16 (3) (2008) 394–400
2. C. M. R. Prado; N. R. Antoniosi Filho. Production and characterization of the biofuels obtained by thermal cracking and thermal catalytic cracking of vegetable oils. *J. Anal. Appl. Pyrolysis*. 86 (2009) 338–347
3. E. Vonghia; D. G. B. Boocock; S. K. Konar, A. Leung. Pathways for the deoxygenation of triglycerides to aliphatic hydrocarbons over activated alumina. *Energy & Fuels*. 9 (1995)1090–1096
4. X. Junming; J. Jianchun; S. Yunjuan, C. Jie. Production of hydrocarbon fuels from pyrolysis of soybean oils using a basic catalyst. *Bioresource Technology*. 101 (2010) 9803–9806
5. N. Taufiqurrahmi; S. Bhatia. Catalytic cracking of edible and non-edible oils for the production of biofuels. *Energy Environ. Sci*. 4 (2011) 1087–1112
6. E. Buzetzkí; K. Sidorová; Z. Cvengrošová; J. Cvengroš. Effects of oil type on products obtained by cracking of oils and fats. *Fuel Processing Technology*. 92 (2011) 2041–2047
7. E. Buzetzkí; K. Sidorová; Z. Cvengrošová; A. Kaszonyi; J. Cvengroš. The influence of zeolite catalysts on the products of rapeseed oil cracking. *Fuel Processing Technology*. 92 (2011) 1623–1631
8. F. Yu; L. Gao; W. Wang; G. Zhang; J. Ji. Bio-fuel production from the catalytic pyrolysis of soybean oil over Me-Al-MCM-41 (Me = La, Ni or Fe) mesoporous materials. *J. Anal. Appl. Pyrolysis*. 104 (2013) 325–329
9. V. P. Doronin; O. V. Potapenko; P. V. Lipin; T. P. Sorokina. Catalytic cracking of vegetable oils and vacuum gas oil. *Fuel*. 106 (2013) 757–765
10. S. A. P. Mota; A. A. Mancio, D. E. L. Lhamas, D. H. de Abreu, M. S. da Silva, W. G. dos Santos, D. A. R. de Castro, R. M. de Oliveira, M. E. Araújo, L. E. P. Borges, N. T. Machado. Production of green diesel by thermal catalytic

- cracking of crude palm oil (*Elaeis guineensis* Jacq) in a pilot plant. *Journal of Analytical and Applied Pyrolysis*. 110 (2014) 1–11
11. Farouq A. Twaiq; Abdul Rahman Mohamed; Subhash Bhatia. Liquid hydrocarbon fuels from palm oil by catalytic cracking over aluminosilicate mesoporous catalysts with various Si/Al ratios. *Microporous and Mesoporous Materials*, Vol. 64, Issues 1–3, 2003, 95–107
 12. Fadouq A. Twaiq; Noor A. M. Zabidi; Subhash Bhatia. Catalytic Conversion of Palm Oil to Hydrocarbons: Performance of Various Zeolite Catalysts. *Ind. Eng. Chem. Res.*, 1999, 38(9), 3230-3237
 13. Farouq A.A Twaiq; A.R Mohamad; Subhash Bhatia. Performance of composite catalysts in palm oil cracking for the production of liquid fuels and chemicals. *Fuel Processing Technology*, Vol. 85, Issue 11, 2004, 1283–1300
 14. Dessy Y. Siswanto; Giyanto W. Salim; Nico Wibisono; Herman Hindarso; Yohanes Sudaryanto; Suryadi Ismadji. Gasoline Production from Palm Oil via Catalytic Cracking using MCM41: Determination of Optimum Conditions. *Journal of Engineering and Applied Sciences*, Vol.3, N° 6, 2008, 42-46
 15. Ooi Yean Sang. Biofuel Production from Catalytic Cracking of Palm Oil. *Energy Sources*, Vol. 25, Issue 9, 2003, 859-869
 16. Mâncio, A.A.; da Costa, K. M. B.; Ferreira, C. C.; Santos, M. C.; Lhamas, D. E. L.; da Mota, S. A. P.; Leão, R. A. C.; de Souza, R. O. M. A.; Araújo, M. E.; Borges, L. E. P.; Machado, N. T. Process analysis of physicochemical properties and chemical composition of organic liquid products obtained by thermochemical conversion of palm oil. *Journal of Analytical and Applied Pyrolysis*, 123 (2017), 284-295
 17. A. A. Mancio; K. M. B. da Costa; C. C. Ferreira; M. C. Santos; D. E. L. Lhamas; S. A. P. da Mota; R. A. C. Leão; R. O. M. A. de Souza; M. E. Araújo; L. E. P. Borges; N. T. Machado. Thermal catalytic cracking of crude palm oil at pilot scale: Effect of the percentage of Na_2CO_3 on the quality of biofuels. *Industrial Crops and Products*, Volume 91, 30 November 2016, 32-43
 18. L. Dandik; H. A. Aksoy, A. Erdem-Senatalar. Catalytic Conversion of Used Oil to Hydrocarbon Fuels in a Fractionating Pyrolysis Reactor. *Energy & Fuels*.12 (1998) 1148–1152
 19. Dandik, L.; Aksoy, H. A. Pyrolysis of used sunflower oil in the presence of sodium carbonate by using fractionating pyrolysis reactor. *Fuel Processing Technology*. Vol.57 (2), 81-92, 1998
 20. L. Li; K. Quan; J. Xu; F. Liu; S. Liu; S. Yu; C. Xie; B. Zhang; X. Ge. Liquid Hydrocarbon Fuels from Catalytic Cracking of Waste Cooking Oils Using Basic Mesoporous Molecular Sieves $\text{K}_2\text{O}/\text{Ba}-\text{MCM}-41$ as Catalysts. *ACS Sustainable Chem. Eng.* 1 (11) (2013) 1412–1416
 21. Ooi Y. S.; Zakaria R.; Mohamed A. R.; Bhatia S. 2004c. Catalytic Cracking of Used Palm Oil and Palm Oil Fatty Acids Mixture for the Production of Liquid Fuel: Kinetic Modeling. *J. Am. Chem. Soc.* 18: 1555-1561
 22. Witchakorn Charusiri; Tharapong Vitidsant. Kinetic Study of Used Vegetable Oil to Liquid Fuels over Sulfated Zirconia. *Energy Fuels*, 2005, 19 (5), 1783–1789
 23. L. Dandik; H. A. Aksoy. Effect of catalyst on the pyrolysis of used oil carried out in a fractionating pyrolysis reactor. *Renew. Energy*. 16 (1–4) (1999) 1007–1010
 24. Ooi Y. S.; Zakaria R.; Mohamed A. R.; Bhatia S. Synthesis of Composite Material MCM-41/Beta and Its Catalytic Performance in Waste Used palm Oil Cracking. *Applied Catalysis A: General*, Volume 274, Issues 1–2, 2004, 15–23
 25. W. H. Chang; C. T. Tye. Catalytic Cracking of Used Palm Oil Using Composite Zeolite. *The Malaysian Journal of Analytical Sciences*, Vol 17 No 1 (2013), 176-184
 26. B. Weber; E. A. Stadlbauer; S. Eichenauer; A. Frank; D. Steffens.; S. Elmar; S. Gerhard. Characterization of Alkanes and Olefins from Thermo-Chemical Conversion of Animal Fat. *Journal of Biobased Materials and Bioenergy*, Vol. 8, N° 5, 2014, 526-537 (12)
 27. S. Eichenauer; B. Weber; E. A. Stadlbauer. Thermochemical Processing of Animal Fat and Meat and Bone Meal to Hydrocarbons based Fuels. *ASME 2015, 9th International Conference on Energy Sustainability*, Paper N° ES2015-49197, V001T02A001, doi: 10.1115/ES2015-49197
 28. Bernd Weber; Ernst A. Stadlbauer; Sabrina Stengl; Mohammad Hossain; Andreas Frank, Diedrich Steffens; Elmar Schlich; Gerhard Schilling. Production of hydrocarbons from fatty acids and animal fat in the presence of water and sodium carbonate. Reactor performance and fuel properties. *Fuel* 94 (2012) 262–269
 29. S. Wang, Z. Guo; Q. Cai; L. Guo. Catalytic conversion of carboxylic acids in bio-oil for liquid hydrocarbons production. *Biomass Bioenergy*. 45 (2012) 138–143
 30. P. Bielansky; A. Weinert; C. Schönberger; A. Reichhold. Gasoline and gaseous hydrocarbons from fatty acids via catalytic cracking. *Biomass Conv, Bioref.* 2 (2012) 53–61
 31. Ooi Y. S; Ridzuan Zakaria; Abdul Rahman Mohamed; Subhash Bhatia. Catalytic conversion of palm oil-based fatty acid mixture to liquid fuel. *Biomass and Bioenergy*, Vol. 27, Issue 5, 2004, 477-484

32. Ooi Y. S., Zakaria R., Mohamed A. R., Bhatia S. Catalytic Conversion of Fatty Acids Mixture to Liquid Fuels over Mesoporous Materials. *Reaction Kinetics Mechanisms and Catalysis Letters* 84, 295-302
33. Ooi Y. S.; Zakaria R.; Mohamed A. R.; Bhatia S. 2005b. Catalytic Conversion of Fatty Acids Mixture to Liquid Fuel and Chemicals over Composite Microporous/Mesoporous Catalysts. *Energy Fuels*, 2005, 19 (3), 736–743
34. Hanna Lappi; Raimo Alén. Production of vegetable oil-based biofuels-Thermochemical behavior of fatty acid sodium salts during pyrolysis. *J. Anal. Appl. Pyrolysis* 86 (2009) 274–280
35. Santos, M. C.; Lourenço, R. M.; de Abreu, D. H.; Pereira, A. M.; de Castro, D. A. R.; Pereira, M. S.; Almeida, H. S.; Mâncio, A. A.; Lhamas, D. E. L.; da Mota, S. A. P.; da Silva Souza, J. A.; Junior, S. D.; Araújo, M. E.; Borges, L. E. P.; Machado, N.T. Gasoline-like hydrocarbons by catalytic cracking of soap phase residue of neutralization process of palm oil (*Elaeis guineensis* Jacq). *Taiwan Institute of Chemical Engineers. Journal*, 71 (2016), 106-119
36. H. da Silva Almeida, O. A. Correa, J. G. Eid, H. J. Ribeiro, D. A. R. de Castro, M. S. Pereira, L. M. Pereira, A. de Andrade Mancio, M. C. Santos, J. A. da Silva Souza, Luiz E. P. Borges, N. M. Mendonca, N. T. Machado. Production of Biofuels by Thermal Catalytic Cracking of Scum from Grease Traps in Pilot Scale. *Journal of Analytical and Applied Pyrolysis* 118 (2016) 20–33
37. H. da Silva Almeida, O.A. Corrêa, J.G. Eid, H.J. Ribeiro, D.A.R. de Castro, M.S. Pereira, L.M. Pereira, A. de Andrade Mâncio, M.C. Santos, S.A.P da Mota, J.A. da Silva Souza, Luiz E.P. Borges, N.M. Mendonça, N.T. Machado. Performance of thermochemical conversion of fat, oils, and grease into kerosene-like hydrocarbons in different production scales. *Journal of Analytical and Applied Pyrolysis*, doi:10.1016/j.jaap.2016.04.017
38. H. da Silva Almeida, O.A. Corrêa, C. C. Ferreira, H. J. Ribeiro, D. A. R. de Castro, M. S. Pereira, A. de Andrade Aâncio, M.C. Santos, S.A.P da Mota, J.A. da Silva Souza, Luiz E.P. Borges, N.M. Mendonça, N.T. Machado. Diesel-like hydrocarbon fuels by catalytic cracking of fats, oils, and grease (FOG) from grease traps. *Journal of the Energy Institute*, doi: 10.1016/j.joei.2016.04.008
39. K. D. Maher, D. C. Bressler. Pyrolysis of triglyceride materials for the production of renewable fuels and chemicals. *Bioresour Technol.* 98 (2007) 2351–2368
40. D. Konwer; S. E. Taylor; B. E. Gordon; J. W. Otvos; M. Calvin. Liquid fuels from *Mesua ferrea* L. seed oil. *JAOCS*. 66 (2) (1989) 223–226
41. Gómez, J. M.; Romero, M. D.; Callejo, V. Heterogeneous basic catalysis for upgrading of biofuels. *Catalysis Today*, v. 218-219, pp. 143-147, 2013.
42. S. Yan; C. Dimaggio; H. Wang; S. Mohan; M. Kim; L. Yang; S. O. Salley; K. Y. Simon Ng. Catalytic Conversion of Triglycerides to Liquid Biofuels Through Transesterification, Cracking, and Hydrotreatment Processes. *Current Catalysis*. 1 (2012) 41–51
43. Pankaj K. Kanaujia; Desavath V. Naik; Deependra Tripathi; Raghuvir Singh; Mukesh K. Poddar; L.N. Siva Kumar Konathala; Yogendra K. Sharma. Pyrolysis of *Jatropha Curcas* seed cake followed by optimization of liquid–liquid extraction procedure for the obtained bio-oil. *Journal of Analytical and Applied Pyrolysis*, Vol. 118, March 2016, 202–224
44. Andréia de Andrade Mâncio. Production, Fractionation and De-acidification of Biofuels Obtained by Thermal Catalytic Cracking of Vegetable Oils. PhD Thesis, Graduate Program of Natural Resources Engineering, April 2015, UFPA, CDD 22, Ed. 660.2995, <http://proderna.propesp.ufpa.br/ARQUIVOS/teses/Andreia.pdf>
45. Ferreira, C. C.; Costa, E. C.; de Castro, D. A. R.; Pereira, M. S.; Mânio, A. A.; Santos, M. C.; Lhamas, D. E. L.; Mota, S. A. P.; Leão, A. C.; Duoisin, S. J; Araújo, M. E.; Borges, L. E. P.; Mahado, N. T. Deacidification of organic liquid products by fractional distillation in laboratory and pilot scales. *Journal of Analytical and Applied Pyrolysis*, 127 (2017), 468-489
46. Mâncio, A. A.; Mota, S. A. P.; Ferreira, C. C.; Carvalho, T. U. S.; Neto, O.; Zamian, J. R.; Araújo, M. E.; Borges, L. E. P.; Machado, N.T. Separation and characterization of biofuels in the jet fuel and diesel fuel ranges by fractional distillation of organic liquid products. *Fuel*, 215 (2018), 212-225
47. Zuo-gang Guo; Shu-rong Wang; Ying-ying Zhu; Zhong-yang Luo; Ke-fa Cen. Separation of acid compounds for refining biomass pyrolysis oil. *Journal of Fuel Chemistry and Technology*, Volume 37, Issue 1, February 2009, 49–52
48. X Guo, S Wang; Z Guo; Q Liu; Z Luo, K Cen. Pyrolysis characteristics of bio-oil fractions separated by molecular distillation. *Applied Energy*, Volume 87, Issue 9, September 2010, 2892-2898
49. Z Guo; S Wang; Y Gu, G Xu; X Li, Z Luo. Separation characteristics of biomass pyrolysis oil in molecular distillation. *Separation and Purification Technology*, Volume 76, Issue 1, 1 December 2010, 52-57
50. Shurong Wang; Yueling Gu; Qian Liu; Yan Yao; Zuogang Guo; Zhongyang Luo; Kefa Cen. Separation of bio-oil by molecular distillation. *Fuel Processing Technology*, Volume 90, Issue 5, May 2009, 738-745

51. Yurong Wang; Shurong Wang; Furong Leng; Junhao Chen; Lingjun Zhu; Zhongyang Luo. Separation and characterization of pyrolytic lignins from the heavy fraction of bio-oil by molecular distillation. *Separation and Purification Technology*, Volume 152, 25 September 2015, 123-132
52. Earl D. Christensen; Gina M. Chupka; Jon Luecke; Tricia Smurthwaite; Teresa L. Alleman; Kristiina Iisa; James A. Franz; Douglas C. Elliott; Robert L. McCormick. Analysis of Oxygenated Compounds in Hydrotreated Biomass Fast Pyrolysis Oil Distillate Fractions. *Energy Fuels*, 2011, 25 (11), 5462–5471
53. S.-Q. Li; Q. Yao; Y. Chi; J.-H. Yan; K.-F. Cen. Pilot-Scale Pyrolysis of Scrap Tires in a Continuous Rotary Kiln Reactor. *Ind. Eng. Chem. Res.* 2004, 43, 5133-5145
54. Ji-Lu Zheng; Qin Wie. Improving the quality of fast pyrolysis bio-oil by reduced pressure distillation. *Biomass and Bioenergy* 35 (2011) 1804-1810
55. Xue-Song Zhang; Guang-Xi Yang; Hong Jiang; Wu-Jun Liu; Hong-Sheng Ding. Mass production of chemicals from biomass-derived oil by directly atmospheric distillation coupled with co-pyrolysis. *SCIENTIFIC REPORTS* | 3: 1120 | DOI: 10.1038/srep01120
56. Anil Kumar Sarma; D. Konwer. Feasibility Studies for Conventional Refinery Distillation with a (1:1) w/w of a Biocrude Blend with Petroleum Crude Oil. *Energy Fuels*, 2005, 19 (4), 1755–1758
57. Yaseen Elkasabi; Charles A. Mullen; Akwasi A. Boateng. Distillation and Isolation of Commodity Chemicals from Bio-Oil Made by Tail-Gas Reactive Pyrolysis. *Sustainable Chem. Eng.* 2014, 2, 2042–2052
58. Vispute, T. P.; Huber, G. W. Production of hydrogen, alkanes and polyols by aqueous phase processing of wood-derived pyrolysis oils. *Green Chem.* 11, 1433–1445 (2009)
59. Shurong Wang; Yurong Wang; Qinjie Cai; Xiangyu Wang; Han Jin; Zhongyang Luo. Multi-step separation of monophenols and pyrolytic lignins from the water-insoluble phase of bio-oil. *Separation and Purification Technology*, Volume 122, 10 February 2014, 248-255
60. Machado, N.T. Fractionation of PFAD-Compounds in Countercurrent Columns Using Supercritical Carbon Dioxide as Solvent. Doctoral Thesis, TU-Hamburg-Harburg, 1998
61. Brunner, G. Industrial Process Development Countercurrent Multistage Gas Extraction (SFE) Processes. *The Journal of Supercritical Fluids* 13 (1998), 283-301
62. Brunner, G. Counter-current separations. *The Journal of Supercritical Fluids*. Volume 47, Issue 3, January 2009, 574-582
63. Poina, M.; Mincione, A.; Gionfrido, F.; Castaldo, D. Supercritical carbon dioxide separation of bergamot essential oil by a countercurrent process. *Flavour and Fragrance Journal*, 2003, 18, 429-435
64. Reverchon, E.; Marciano, A.; Poleto, M. Fractionation of a peel oil key mixture by supercritical CO₂ in a continuous tower: *Industrial & Engineering Chemistry Research*, 1997, 36, 4940-4948
65. Sato, M.; Kondo, M.; Goto, M.; Kodama, A.; Hirose, T. Fractionation of citrus oil by supercritical countercurrent extractor with side-stream withdrawal. *Journal of Supercritical Fluids*, 1998, 13, 311-317.
66. Kondo, M.; Goto, M.; Kodama, A.; and Hirose, T. Separation performance of supercritical carbon dioxide extraction columns for the citrus oil processing: observation using simulator. *Separation Science and Technology*, 2002, 37, 3391- 3406
67. Danielski, L.; Brunner, G.; Schwanke, C.; Zetzl, C.; Hense, H.; Donoso, J.P.M. Deterpenation of mandarin (*Citrus reticulata*) peel by means of countercurrent multistage extraction adsorption/desorption with supercritical CO₂. *Journal of Supercritical Fluids*, Volume 44, Issue 3, Apr 2008, 315-324
68. Budich, M.; Heilig, S.; Wesse, T.; Leibkuchler, V.; Brunner, G. Countercurrent deterpenation of citrus oils with supercritical CO₂. *Journal of Supercritical Fluids*, Volume 14, Issue 2, Jan 1999, 105-114
69. Simoes P. C; Matos H. A; Carmelo P. J; Gomes de Azevedo E; Nunes da Ponte M. Mass transfer in countercurrent packed columns—application to supercritical CO₂ extraction of terpenes. *Ind Eng Chem Res* 1995;34(2):613-618.
70. Pedro C. Simoes, Henrique A. Matos, Paulo J. Carmelo, Edmundo Gomes de Azevedo, Manuel Nunes da Ponte. Mass Transfer in Countercurrent Packed Columns: Application to Supercritical CO₂ Extraction of Terpenes. *Ind. Eng. Chem. Res.*, 1995, 34 (2), 613–618
71. Shohei Yasumoto, Armando T. Quitain, Mitsuru Sasaki, Hideo Iwai, Masahiro Tanaka, Munehiro Hoshino. Supercritical CO₂-mediated countercurrent separation of essential oil and seed oil. *The Journal of Supercritical Fluids*, Volume 104, September 2015, 104-111
72. Benvenuti, F.; Gironi, F.; Lamberti, L. Supercritical Deterpenation of Lemon Essential Oil, *Experimental Data and Simulation of Semicontinuous Extraction Process*. *The Journal of Supercritical Fluids* 20 (2001), 29-44
73. Fleck, U.; Tiegs, C.; Brunner, G. Fractionation of fatty acid ethyl esters by supercritical CO₂: high separation efficiency using an automated countercurrent column. *Journal of Supercritical Fluids*, Volume 14, Issue 1, Oct 1998, 67-74

74. Riha, V.; Brunner, G. Separation of fish oil ethyl esters with supercritical carbon dioxide. *Journal of Supercritical Fluids*, Volume 17, Issue 1, Feb 2000, 55-64
75. Torres C. F.; Torrello G.; Señoráns F. J.; Reglero G. Supercritical fluid fractionation of fatty acid ethyl esters from buteroil. *J Dairy Sci.* 2009 May;92(5):1840-1845
76. Eduardo G. Cervo; Sourabh U. Kulkarni; Mark C.Thies. Isolating polycyclic aromatic hydrocarbon (PAH) oligomers via continuous, two-column supercritical extraction. *The Journal of Supercritical Fluids*, Volume 66, June 2012, 120-128
77. Señoráns F. J.; Ruiz-Rodríguez A.; Cavero S.; Cifuentes A.; Ibañez E.; Reglero G. Isolation of antioxidant compounds from orange juice by using countercurrent supercritical fluid extraction (CC-SFE). *J Agric Food Chem.* 2001 Dec;49(12):6039-6044
78. Simó C.; Ibañez E.; Señoráns F. J.; Barbas C.; Reglero G.; Cifuentes A. Analysis of antioxidants from orange juice obtained by countercurrent supercritical fluid extraction, using micellar electrokinetic chromatography and reverse-phase liquid chromatography. *J Agric Food Chem.* 2002 Nov 6;50(23):6648-6652
79. Simoes, P. C.; Carmelo, P. J.; Pereira, P. J.; Lopes, J. A.; da Ponte, M. N.; Brunner, G. Quality assessment of refined olive oils by gas extraction. *Journal of Supercritical Fluids*, Volume 13, Issue 1-3, Jun 1998, 337-341 (deacidification of olive oil)
80. Dunford, N.T.; Teel, J.A.; King, J.W., A continuous countercurrent supercritical fluid deacidification process for phytosterol ester fortification in rice bran oil. *Food Research International*, 2003, 36, 175-181 (deacidification of rice bran oil)
81. Tiziana Fornari; Luis Vázquez; Carlos F. Torres; Elena Ibañez; Francisco J. Señoráns; Guillermo Reglero. Countercurrent supercritical fluid extraction of different lipid-type materials: Experimental and thermodynamic modeling. *The Journal of Supercritical Fluids*, Volume 45, Issue 2, June 2008, 206-212
82. Vásquez, L.; Benavides-Hurtado; A. M., Reglero, G.; Fornari, T.; Ibañez, E., Senorans, F.J. Deacidification of Olive Oil by Countercurrent Supercritical Carbon Dioxide Extraction: Experimental and Thermodynamic Modeling. *Journal of Food Engineering* 90 (2009), 463-470
83. Machado, N.T.; Brunner, G. Separation of Saturated and Unsaturated Fatty Acids from Palm Fatty Acids Distillates in Continuous Multistage Countercurrent Columns with Supercritical Carbon Dioxide as Solvent: A Process Design Methodology. *Ciência e Tecnologia de Alimentos.* 17(4), 361-370, 1997
84. G. Brunner; N. T. Machado. Process design methodology for fractionation of fatty acids from palm fatty acid distillates in countercurrent packed columns with supercritical CO₂. *The Journal of Supercritical Fluids*, Volume 66, June 2012, 96-110
85. Vásquez, L.; Torres, C. F.; Fornari, T.; Senórans, F. J.; Reglero, G. Recovery of Squalene from Vegetable Oil Sources Using Countercurrent Supercritical Carbon Dioxide Extraction. *Journal of Supercritical Fluids* 40 (2007), 59-66
86. Gast, K.; Jungfer, M.; Saure, C.; Brunner, G. Purification of tocochromanols from edible oil. *Journal of Supercritical Fluids*, Volume 34, Issue 1, May 2005, 17-25.
87. G. Brunner; Th. Malchow; K. Stürken; Th. Gottschau. Separation of tocopherols from deodorizer condensates by countercurrent extraction with carbon dioxide. *The Journal of Supercritical Fluids*, Volume 4, Issue 1, March 1991, 72-80
88. Bondioli, P., C. Mariani, A. Lanzani, E. Fedeli, and A. Muller, Squalene Recovery from Olive Oil Deodorizer Distillates, *J. Am. Oil Chem. Soc.* 70:763-766 (1993)
89. Elena Ibañez, Andrés M. Hurtado Benavides, Francisco J. Señoráns, Guillermo Reglero. Concentration of sterols and tocopherols from olive oil with supercritical carbon dioxide. *Journal of the American Oil Chemists' Society*, December 2002, Volume 79, Issue 12, 1255-1260
90. Tabera J; Guinda A; Ruiz-Rodríguez A; Señoráns F. J, Ibañez E; Albi T; Reglero G. Countercurrent supercritical fluid extraction and fractionation of high-added-value compounds from a hexane extract of olive leaves. *J Agric Food Chem.* 2004 Jul 28;52(15):4774-4779
91. Señoráns F. J; Ruiz-Rodríguez A; Ibañez E; Tabera J; Reglero G. Countercurrent supercritical fluid extraction and fractionation of alcoholic beverages. *J Agric Food Chem.* 2001 Apr;49(4):1895-1899
92. Senorans F. J; Ruiz Rodriguez A; Ibañez E; Tabera J; Reglero G. Optimization of countercurrent supercritical fluid extraction conditions for spirits fractionation. *J Supercrit Fluids* 2001; 21:41-49
93. Budich, M.; Brunner, G. Supercritical fluid extraction of ethanol from aqueous solutions. *Journal of Supercritical Fluids*, Volume 25, Issue 1, Jan 2003, 45-55
94. Arturo Bejarano; José M.del Valle. Countercurrent fractionation of aqueous apple aroma constituents using supercritical carbon dioxide. *The Journal of Supercritical Fluids*, Volume 120, Part 2, February 2017, 266-274

95. Senorans F. J; Ruiz Rodríguez A; Ibáñez E; Tabera J; Reglero G. Isolation of brandy aroma by countercurrent supercritical fluid extraction. *J Supercrit Fluids* 2003;26:129-135
96. Sofia Macedo, Susana Fernandes, José A. Lopes; Hermínio C. de Sousa; Paulo J. Pereira; Paulo J. Carmelo; Carlos Menduiña; Pedro C. Simões, Manuel Nunes da Ponte. Recovery of Wine-Must Aroma Compounds by Supercritical CO₂. *Food Bioprocess Technol* (2008) 1:74-81
97. Vázquez L; Fornari T; Señoráns F. J; Reglero G, Torres CF. Supercritical carbon dioxide fractionation of nonesterified alkoxyglycerols obtained from shark liver oil. *J Agric Food Chem.* 2008 Feb 13;56(3):1078-83
98. Rui Ruivo, Maria J. Cebola, Pedro C. Simões, M. Nunes da Ponte. Fractionation of Edible Oil Model Mixtures by Supercritical Carbon Dioxide in a Packed Column. Part I: Experimental Results. *Ind. Eng. Chem. Res.*, 2001, 40 (7), 1706–1711
99. Rui Ruivo, M. João Cebola, Pedro C. Simões, M. Nunes da Ponte. Fractionation of Edible Oil Model Mixtures by Supercritical Carbon Dioxide in a Packed Column. 2. A Mass-Transfer Study. *Ind. Eng. Chem. Res.*, 2002, 41 (9), 2305–2315
100. João Fernandes; Rui Ruivo; Pedro Simões. Dynamic model of a supercritical fluid extraction plant. *AIChE Journal*, April 2007, Volume 53, Issue 4, 752–763
101. J. Fernandes; J. P. B. Mota; P. Simões. Non-isothermal dynamic model of a supercritical fluid extraction packed column. *The Journal of Supercritical Fluids*, Volume 41, Issue 1, May 2007, 20-30
102. Arturo Bejarano, Pedro C. Simões, José M. del Valle. Fractionation technologies for liquid mixtures using dense carbon dioxide. *The Journal of Supercritical Fluids*, Volume 107, January 2016, 321-348
103. Moricet, M. Simulierung von Gasextraktion in Bodenkolumnen am Beispiel der Abtrennung von Monoglycerid aus einen Ölsäureglyceridgemisch sowie der Freien Fettsäure aus Palmöl. Doctoral Thesis, Universität Erlagen-Nürnberg, 1982
104. *Simoës, P. C.; Brunner, G.* Multicomponent phase equilibria of an extra-virgin olive oil in supercritical carbon dioxide. *Journal of Supercritical Fluids*, Volume 9, Issue 2, Jun 1996, 75-81
105. Mendes, M. F; Uller, A. M. C; Pessoa, F. L. P. Simulation and Thermodynamic Modeling of The Extraction of Tocopherol from a Synthetic Mixture of Tocopherol, Squalene and CO₂. *Brazilian Journal of Chemical Engineering* 17 (4-7), 761-770, 2000
106. Mendes, M. F.; Pessoa, Fernando Luiz Pellegrini ; Uller, Angela Maria Cohen. Study of the Phase Equilibrium between carbon dioxide and the deodorizer distillate of the soybean oil. *Chemical Engineering Transactions*, Italy, Vol. 2, 351-356, 2002
107. Benvenuti, F.; Gironi, F.; Lamberti, L. Supercritical Deterpenation of Lemon Essential Oil, Experimental Data and Simulation of Semicontinuous Extraction Process. *The Journal of Supercritical Fluids* 20 (2001), 29-44
108. E. B. de Moraes; Mario E. T. Alvarez; M. R. W. Maciel; R. M. Filho. Simulation and optimization of a supercritical extraction process for recovering provitamin A. *Applied Biochemistry and Biotechnology*, March 2006, Volume 132, Issue 1–3, 1041–1050
109. da Silva, H. V. Modelagem e Simulação do Fracionamento de Correntes Líquidas de Produtos Naturais em Colunas em Contracorrente Usando Dióxido de carbono Supercrítico. Master Thesis, Faculty of Chemical Engineering, UFPA, Belém-Pará-Brazil, 2011, <http://ppgeq.prosp.ufpa.br/ARQUIVOS/dissertacoes/Hermann%20da%20Silva%20Vargens.pdf>
110. Fernandes, J.B.; Lisboa, P.F.; Mota, J.P.B.; Simões, P.C. Modelling and simulation of a complete supercritical fluid extraction plant with countercurrent fractionation column. *Separation Science and Technology*, Volume 46, Issue 13, August 2011, Pages 2088-2098
111. Carlos Ariel Pieck; Christelle Crampon; Frédéric Charton; Elisabeth Badens. Multi-scale experimental study and modeling of the supercritical fractionation process. *The Journal of Supercritical Fluids*, Volume 105, October 2015, 158-169
112. E. C. Costa; C. C. Ferreira; A. L. B. dos Santos; H. da Silva Vargens; E. G. O. Menezes; V. M. B. Cunha; M. P. da Silva; A. A. Mâncio; N.T. Machado; M. E. Araújo. Process simulation of organic liquid products fractionation in countercurrent multistage columns using CO₂ as solvent with Aspen-HYSYS. *J. of Supercritical Fluids* 140 (2018) 101–115
113. Elinéia Castro Costa, Welisson de Araújo Silva, Eduardo Gama Ortiz Menezes, Marcilene Paiva da Silva, Vânia Maria Borges Cunha, Andréia de Andrade Mâncio, Marcelo Costa Santos, Sílvio Alex Pereira da Mota, Marilena Emmi Araújo, Nélio Teixeira Machado. Simulation of Organic Liquid Products Deoxygenation by Multistage Countercurrent Absorber/Stripping Using CO₂ as Solvent with Aspen-HYSYS: Thermodynamic Data Basis and EOS Modeling. *Molecules* 2021, 26, 4382. <https://doi.org/10.3390/molecules26144382>

114. R. Jimenez-Gallegos, L.A. Galicia-Luna, O. Elizalde-Solis, Experimental vapor-liquid equilibria for the carbon dioxide + octane and carbon dioxide + decane systems. *J. Chem. Eng. Data* 51 (2006) 1624–1628
115. L.E. Camacho-Camacho, L.A. Galicia-Luna, O. Elizalde-Solis, Z. Martinez-Ramirez. New isothermal vapor-liquid equilibria for the CO₂ + n-nonane, and CO₂ + n-undecane systems. *Fluid Phase Equilibria*, 259 (2007) 45–50
116. K.A.M. Gasem, K.B. Dickson, P.B. Dulcamara, N. Nagarajan, R.L.J. Robinson. Equilibrium phase compositions, phase densities, and interfacial tensions for CO₂ + hydrocarbon systems, CO₂ + n-Tetradecane. *J. Chem. Eng. Data* (1989) 191–195
117. C. Secuianu, V. Feroiu, D. Geană. Phase behavior for the carbon dioxide + Npentadecane binary system. *J. Chem. Eng. Data* 55 (2010) 4255–4259
118. R. D'Souza, J.R. Patrick, A.S. Teja. High-pressure phase equilibria in the carbon dioxide-n-hexadecane and carbon dioxide-water systems. *Can. J. Chem. Eng.* 66 (1988) 319
119. J.S. Yau, Y.Y. Chiang, D.S. Shy, F.N. Tsai. Solubilities of carbon dioxide in carboxylic acids under high pressures. *J. Chem. Eng. Jpn.* 25 (5) (1992) 544–548
120. R. Bharath, H. Inomata, T. Adschiri, K. Arai. Phase equilibrium study for the separation and fractionation of fatty oil components using supercritical carbon dioxide. *Fluid Phase Equilibria*, 81 (1992) 307–320
121. Raganath Bharath, Seichiro Yamane, Hiroshi Inomata, Tadafumi Adschiri, Kunio Arai. Phase Equilibria of Supercritical CO₂-Fatty oil Component Binary Systems. *Fluid Phase Equilibria*, 83 (1993) 183-192
122. A. A. Mâncio; S. A. P da Mota; L. E. P. Borges; N. T. Machado. Obtaining of green gasoline by fractional distillation of organic liquid products from the thermal-catalytic cracking using different percentages of catalyst. *Scientia Plena* 13, 012711(2017), doi:10.14808/sci.plena.2017.012711